UNIVERSITA' DEGLI STUDI DEL PIEMONTE ORIENTALE
"AMEDEO AVOGADRO"

Dipartimento di Medicina Traslazionale

Corso di Dottorato di Ricerca in Medicina Clinica e Sperimentale

ciclo XXVIII

Vitamin D effects on endothelial cells: novel insights into its extra skeletal properties

SSD (Settore Scientifico Disciplinare) della tesi BIO/9

Coordinatore
Prof.ssa Marisa Gariglio

Tutor
Prof. Claudio Molinari

Dottoranda
Diletta Francesca Squarzanti

INDEX

INTRODUCTION

History of nutrition and rickets

Vitamin D history is quite long and definitely fascinating. It started in early 1900, when Hopkins supposed the existence of a dietary factor that could prevent rickets (1). Rickets appears as a failure of the normal mineralization of growing bones; other signs include short stature, growth retardation and bone deformities (2, 3). In 1919 Mellanby experimented a low-fat diet on dog puppies. They developed rickets, which was prevented by adding cod-liver oil to their diet (4). Mc Collum and coworkers in 1922 showed that heated, oxidized cod-liver oil contained no more vitamin A, but it was still effective for treating rickets (5). This was the key experiment for the discovery of the anti-rickets factor, baptized since that moment "vitamin D", but for the time being without the characterization of its chemical structure. In the meantime, an entirely different process to cure rickets came out: sunlight or UV light irradiation. In the 1920s, Alfred F. Hess revealed that signs of illness rapidly disappeared when rachitic children were exposed to direct sunlight (6). In 1926 Adolf Windaus and coworkers identified the chemical structures of 7-dehydrocholesterol and cholecalciferol, precursors of the active form of vitamin D. Two years later Windaus won the Nobel Prize because of his studies on sterols and vitamins (7, 8).

It is well known nowadays that vitamin D could be introduced from foods and also self-produced by our body through ultraviolet B exposure. Actually the role of vitamin D in preventing rickets depends on its ability to increasing calcium pumps expression to facilitate Ca^{2+} uptake across the intestine (9).

Vitamin D metabolism

Vitamin D intake from diet is limited. The main dietary sources of vitamin D_2 and vitamin D_3 consist of cod liver oil, fishes (such as mackerel, salmon and sardines), mushrooms and egg yolks. Since 1930 vitamin D-fortified foods became popular (milk, margarine, infant formula, cheese, breakfast cereals and orange juice especially in the USA). Vitamin D_2 and D_3 are also available as oral over-the-counter supplements (10-12).

Different organs and intermediates participate to the synthesis of the bioactive form of vitamin D (13-21; Figure 1). First, 7-dehydrocholesterol is photochemical converted to pre-

vitamin D_3 in the stratum basale and stratum spinosum layers of skin by solar radiation (UVB: 290-315 nm) and then it is thermally isomerized to vitamin D_3 (cholecalciferol). This photo-production is influenced by several factors including ethnicity (skin pigmentation), UV exposure (latitude, season, use of sunscreen and clothing), and age. Caucasican and Asian subjects, with a lighter skin pigmentation than African and East Indian populations, are able to produce more vitamin D_3. Increasing age involves the falls in the concentration of 7-dehydrocholesterol, resulting in the reduced capacity to synthesize the bioactive form of vitamin D. Less outdoor activity and unhealthy lifestyle habits are also cause of a lower vitamin D_3 production. Conversely, excessive exposure to sunlight degrades pre-vitamin D_3 and vitamin D_3 into inactive photoproducts.

Three enzymes belonging to cytochrome P450 oxidases (CYPs) perform vitamin D metabolism. They are located either in the endoplasmatic reticulum or in the mitochondria (Figure 2).

Vitamin D-binding protein (DBP) binds cholecalciferol and transport it to the liver, where the first hydroxylation occurs at position 25: the enzyme 25-hydroxylase (CYP27A1, CYP2R1) converts vitamin D3 into 25-hydroxyvitamin D_3 ($25(OH)D_3$ or calcidiol). CYP27A1 is widely distributed in the body, whereas CYP2R1 is primarily expressed in the liver and testes. $25(OH)D_3$ is the major circulating form of vitamin D and its level in the blood is measured to assess a patient's vitamin D status. Alternatively, fat cells could store vitamin D before this first step of activation.

The second hydroxylation occurs at position 1 by the enzyme 1α-hydroxylase (CYP27B1) in the kidney, where the biologically active form of vitamin D ($1,25(OH)_2D_3$ or calcitriol) is produced. Although the kidney is the main source of $1,25(OH)_2D_3$, other tissues could also express this enzyme, such as endothelial cells (ECs), epithelial cells in the skin, lung, breast, intestine, parathyroid glands, cells of the immune system, osteoblasts and chondrocytes. Several factors regulate the renal synthesis of $1,25(OH)_2D_3$, including serum phosphorus and calcium levels, fibroblast growth factor-23 (FGF-23), parathyroid hormone (PTH) and $1,25(OH)_2D_3$ itself, with a feedback regulation to minimize a potential toxic condition.

Finally, 24-hydroxylase (CYP24A1) degrades calcitriol mostly to a biologically inactive metabolite, the calcitroic acid, which is excreted in the bile.

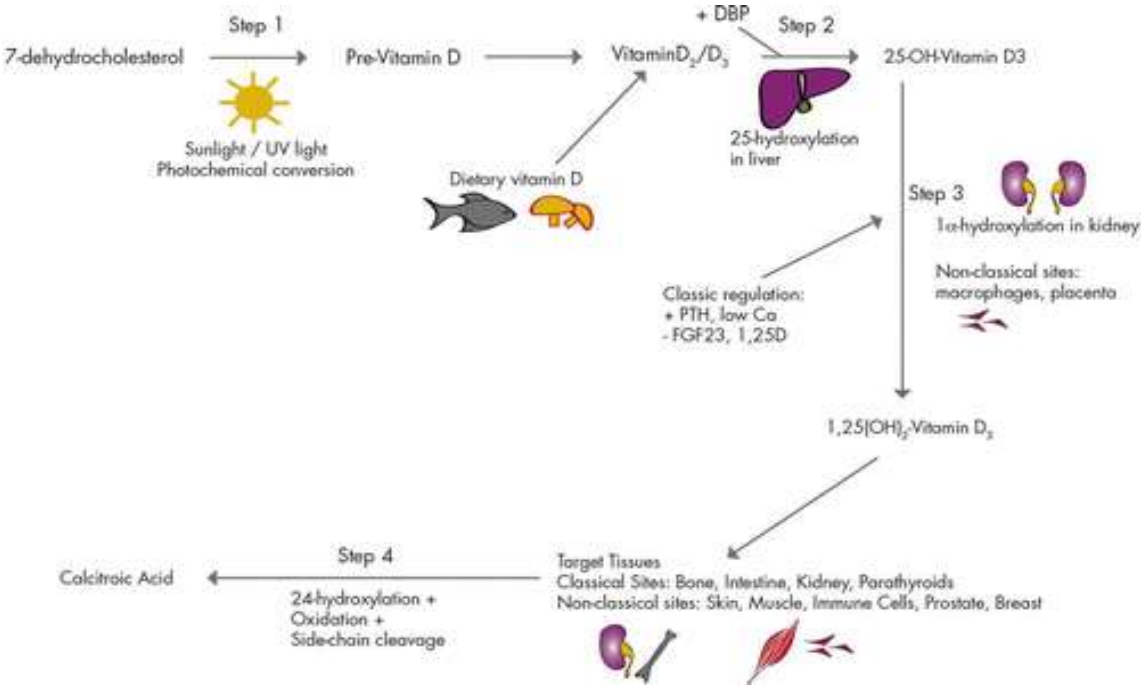

Figure 1. Vitamin D metabolism. Girgis CM et al. Endocrine Reviews. 2013.

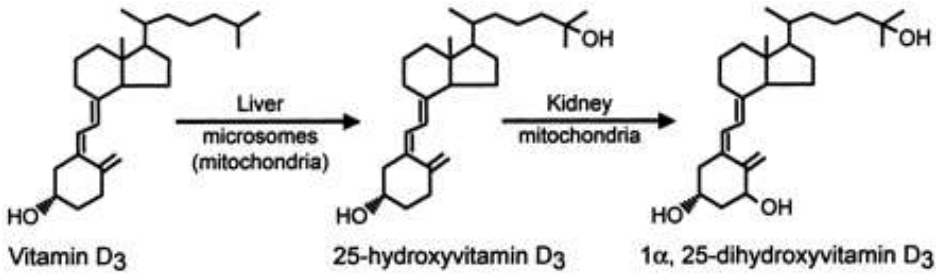

Figure 2. Metabolic activation of vitamin D to its hormonal biologically active form, 1,25(OH)$_2$D$_3$. DeLuca HF et al. Am J Clin Nutr. 2004.

Nuclear vitamin D receptors (VDRs) mediate vitamin D genomic action

Generally vitamin D-induced genomic responses take from hours to days to be fully apparent and can be blocked inhibiting transcription and translation processes. 1,25(OH)$_2$D$_3$ exerts these biological effects within target cells through the binding to Vitamin D Receptor (VDR), a member of the superfamily of hormone-activated nuclear receptors (13). Two distinct functional domains compose the protein, an N-terminal and a C-terminal domain, linked by an unstructured region. The N-terminal is a dual zinc finger DNA-binding domain, while the

C-terminal is the ligand-binding domain (22). The interaction between $1,25(OH)_2D_3$ and VDR causes conformational changes within the receptor, inducing the formation of VDR-VDR homodimers or, preferentially, VDR-RXR (Retinoid X Receptor) heterodimers (23, 24). The ligand-VDR-RXR complex binds to vitamin D responsive elements (VDREs) in the DNA, typically direct repeats of two hexameric binding sites separated by a three base pair spacer. VDR binding to its VDRE recruits coregulatory complexes to carry out its genomic activity. Vitamin D regulates the expression of up to 2000 genes, such as those involved in cell cycle regulation, apoptosis, autophagy and cell adhesion, many of whose promoters contain specific VDREs. In some cases multiple copies of VDREs are positioned not only in the proximal promoter region but also dispersed in the transcription start site of vitamin D-controlled genes (25).

Steroidal nuclear receptors classically complex with heat shock factor proteins in the cytoplasm; the ligand mediates the expression of their transcriptional power, inducing the release from the complex and the translocation into the nucleus. VDR acts differently: it is localized in the nucleus in the presence but also in the absence of the ligand, and has the ability to activate or repress gene expression depending on the availability of the ligand (24). In the absence of the ligand, VDR-RXR heterodimers associates at enhancer and promoter regions with corepressors to silence gene expression (26-30). Instead the binding of the ligand induces formation of a coactivator complex causing target gene transactivation (24). VDR can bind many different proteins with transcriptional activator function (31-33).

Membrane-associated binding proteins mediate vitamin D non-genomic action

Vitamin D could also elicit rapid responses, generated within 1-2 to 15-45 minutes, that do not involve the regulation of gene expression. Cell surface receptors mediate this non-genomic action. The better characterized is the membrane-associated, rapid-response steroid binding protein ($1,25D_3$ MARRS) isolated in basal-lateral membranes of chick intestinal epithelium (34). These receptors directly influence different signaling pathways, such as those involving phosphoinosities, Ca^{2+}, cyclic guanosine monophosphate (cGMP) and mitogen-activated protein (MAP) kinases.

VDR could also mediate rapid responses, but binding to different ligands (6-s-cis) from those used by the classic nuclear VDR, which ligands (6-s-trans) generate genomic responses. Moreover, this kind of VDR is not localized into the nucleus but associated to plasma

membrane lipid-raft caveolae microdomains, as reported for many different tissues and cell types. Caveolae are membrane invaginations enriched in sphingolipids and cholesterol; in those regions, $1,25(OH)_2D_3$ displays the same relative binding affinities to caveolae-associated VDR compared to nuclear VDR (35, 36).

Finally, annexin-II has been proposed for the role of mediator of vitamin D action. This molecule is a membrane-associated binding protein that acts as a calcium-specific ion channel. Baran et al. suggest its ability to bind $1,25(OH)_2D_3$ directly in osteoblasts but a more recent study reports evidence that deny this hypothesis (37, 38).

Non-genomic pathways may cooperate with the classical genomic one, however the mechanisms that mediate vitamin D-induced non-genomic action are not well understood yet.

Vitamin D deficiency

Vitamin D deficiency implies severe consequences in growing children causing rickets, and in adults determining osteomalacia. The clinical symptoms include also myopathy and muscle weakness and pain. The resulting secondary hyperparathyroidism causes an increased osteoclastic activity that leads to mineral bone loss, worsening osteopenia and osteoporosis in adults. Furthermore, the risk of falling and fractures is increased in elderly people (16). Serum concentration of 25-hydroxyvitamin D_3 levels is used by clinicians to determine vitamin D status in the general population, since it reflects both dietary vitamin D intake and endogenous production. Table 1 reports the definitions linked to calcidiol levels, even if no consensus on optimal level has been reached yet (39, 40).

The American Institute of Medicine has revised vitamin D-recommended daily allowance (RDA) in 2010, setting it at 600 IU per day for the general population and at 800 IU per day for people from 70 years up (1 IU is the biological equivalent of 0.025 µg of vitamin D3) (41). Although the knowledge of healthy vitamin D ranges, a discrepancy between the intake and the recommended vitamin D levels still exist. The chronic insufficiency of nutrients without immediately apparent clinical symptoms has been defined “hidden hunger”, and for vitamin D is more recurrent in the developing countries and in elderly people (42).

Moreover, nowadays people are less exposed to UV radiation and it seems that humans are going to progressively lose the ability to synthesize vitamin D, even if exposed to sun light.

Recently a global vitamin D status map has been drawn up, based on a systematic review of the worldwide vitamin D levels, employing all available publications from 1990 to 2011.

Prevalence of hypovitaminosis D has re-emerged as a public health problem, widespread globally (43). Moreover, many studies suggest that low vitamin D level is involved as etiological factor in the pathogenesis of many diseases (hypertension, hyperlipidemia, peripheral vascular disease, coronary artery disease, myocardial infarction, heart failure, stroke, cancer, autoimmune diseases, infections, neurocognitive disorders, type 2 diabetes mellitus and obesity) (43-45). Schöttker and colleagues, for example, analyzed data from eight prospective cohort studies involving both European and American participants (46). They investigated the association between serum 25-hydroxyvitamin D_3 concentration and mortality in more than 26000 men and women aged from 50 to 79 years. The main outcome measures were all-cause, cardiovascular, and cancer mortality. In this meta-analysis, lower vitamin D concentration was associated with increased all-cause mortality, cardiovascular mortality, and cancer mortality (in subjects with a history of cancer). Results were consistent across study populations, sex, age, and seasons of blood draw.

Many data deriving from basic researches and animal models support a protective role of vitamin D against cancer, but the debate remains open regarding humans. Thus VDR is currently the target of many trials whose aim is to investigate its roles in several human health outcomes including cancer, cardiovascular health, and other common disease phenotypes.

$25(OH)D_3 < 20$ ng/ml	Severe deficiency
$25(OH)D_3 = 21$-29 ng/ml	Insufficiency or moderate deficiency
$25(OH)D_3 > 30$ ng/ml	Sufficiency (40-60 ng/ml preferable range)
$25(OH)D_3 > 100$ ng/ml	Overdose
$25(OH)D_3 > 150$ ng/ml	Toxicity

Table 1: Serum calcidiol ranges and related definitions.

Skeletal effects of vitamin D

Vitamin D plays an essential role in calcium and phosphate metabolism and maintains

minerals homeostasis to assure metabolic functions and bone mineralization. The need of the organism is firstly satisfied by dietary calcium and, when this is not sufficient, by calcium mobilization from bone and renal reabsorption. Classical vitamin D-responsive tissues are bones, intestine, kidney and parathyroid glands.

Bone. In order to mobilize skeletal calcium stores. $1,25(OH)_2D_3$ interacts with VDR in osteoblasts, causing an increased expression of the receptor activator of nuclear factor-κB ligand (RANKL). The binding of RANKL to its receptor RANK on pre-osteoclasts induces these cells to mature into osteoclasts, which dissolve the mineralized collagen matrix in bone, maintaining mineral levels in the blood and, when excessive, causing osteopenia, osteoporosis and an enhanced risk of fractures (44, 47).

Intestine. $1,25(OH)_2D_3$ increases the efficiency of intestinal absorption from 10-15 % to 30-40 % for calcium and from 30-40 % to about 80 % for phosphorus, respectively. Moreover, VDR-RXR complex induces the expression of proteins involved in active intestinal calcium absorption, in particular the epithelial calcium channel TRPV6 (transient receptor potential vanilloid type 6) and $calbindin_{9K}$, a calcium-binding protein (CaBP) (45). Following TRPV6 and CaBPs transcellular transport, Ca^{2+} diffuses in the cytosol and is then extruded across the basolateral membrane. In addition a paracellular model within the intercellular spaces involving tight junctions has been proposed (48).

Kidney. In this organ, $1,25(OH)_2D_3$ controls its own concentration, simultaneously inducing 24-hydroxylase and suppressing 1α-hydroxylase expression. Furthermore, it enhances renal Ca^{2+} reabsorption and calbidin expression, and accelerates PTH-dependent Ca^{2+} transport in the distal tube, which determine the final calcium excretion in the urine.

Parathyroid glands. The vitamin D endocrine system is a potent modulator of parathyroid functions, maintain normal parathyroid status and preventing proliferation of parathyroid gland cells. $1,25(OH)_2D_3$ inhibits PTH gene transcription and reduces parathyroid cell proliferation, improving parathyroid hyperplasia. Moreover, it controls VDR levels in the parathyroid glands and their response to calcium. PTH enhances tubular calcium and decreases renal phosphorus reabsorption; moreover it stimulates the kidneys to produce $1,25(OH)_2D_3$ (44, 47). Patients with renal failure becomes vitamin D deficient, since the site of production of $1,25(OH)_2D_3$ is destroyed. If the circulation allows adequate calcium levels, the parathyroid glands hyperproliferate and secretes large amount of PTH, resulting in secondary hyperparathyroidism (49).

Extra skeletal effects of vitamin D

Many tissues respond to vitamin D (among others prostate, breast, immune cells, skeletal muscle, cardiac tissue, parathyroid glands, skin, endothelial cells and brain), express VDR and the enzyme 1α-hydroxylase (Figure 3). The widespread VDR expression also in tissues that do not participate in mineral homeostasis could explain the broad spectrum of vitamin D clinical effects, beyond the bone. Vitamin D exerts its activity through two mechanisms: the hormone signaling, in which the biologically active form reaches target cells through the bloodstream; and the autocrine/paracrine signaling, in which locally produced-1,25$(OH)_2D_3$ affects surrounding cells. Here are reported some examples.

Vitamin D is a potent immunomodulatory. After a skin lesion, keratinocytes, which compose the mucocutaneous barrier, upregulate VDR and 1α-hydroxylase expressions. Monocytes and macrophages act in the same way after a *Mycobacterium tuberculosis* infection or exposition to lipopolysaccharides. An increased cathelicidin and α-defensin 2 production results in all cases and these two proteins could display their antimicrobial effects, promoting innate immunity. It has been hypothesized that monocytes or macrophages may also release self-produced-1,25$(OH)_2D_3$ to act locally on activated T and B lymphocytes, which are able to regulate cytokine and immunoglobulin synthesis, respectively (44, 50).

In cancer cells (such as breast, colon and prostate), 1,25$(OH)_2D_3$-VDR complex regulate genes controlling proliferation; indeed this complex could arrest cells cycle in the G1-G0 transition, inducing p21 and p27 synthesis and/or stabilization, blocking cell growth and promoting cell differentiation. In TGF-α/EGFR dependent tumor, vitamin D could inhibit the growth inducing the recruitment of the activated receptor into early endosomes, reducing growth signaling. It also shows anti-proliferative properties in psoriatic keratinocytes overexpressing TGF-α. In monocytes and osteoblasts culture, it seems that the biologically active form of vitamin D could enhance the expression of a suppressor of the oncogenic cyclin D1, C/EBPβ. Moreover, vitamin D is able to regulate apoptosis. It could induce this process in breast cancer cells for example, where it may modulate Bcl2 and Bax content. But it could also show anti-apoptotic effects, essential in normal tissue development and function. For instance it protects keratinocytes from UV-irradiation or chemotherapy-induced apoptosis and melanocytes from TNF-α-mediated apoptosis. In normal keratinocytes vitamin D induces cell differentiation and maintains a calcium gradient necessary for the integrity of the permeability barrier of the skin. 1,25$(OH)_2D_3$ represses tumor invasion and metastasis

reducing matrix metalloproteinases activity (MMPs) and enhancing the expression of molecules with adhesive properties like E-cadherin.

$1,25(OH)_2D_3$ acts as a negative endocrine regulator of the renin-angiotensin system. Indeed it enters the circulation and can down-regulate renin production and stimulate insulin secretion in the β-islet cells of the pancreas (44, 47).

Vitamin D is thought to possess positive effects on muscle, affecting the calcium handling in the cells and promoting *de novo* protein synthesis. $1,25(OH)_2D_3$ maintains calcium balance in cultured muscle cells initially via inositol triphosphate induced-rapid ion release from the sarcoplasmic reticulum, and then through ion channels that allows calcium influx from the extracellular compartment. Vitamin D deficiency and sarcopenia (age-related loss of muscle mass) are associated with atrophy of mainly type II fibers. Vitamin D supplementation reduces fractures incidence, actually decreasing the number of falling (13, 16).

Vitamin D deficiency is associated with cardiomyopathy and increased risk of cardiovascular disease (CVD) with significant consequent mortality in humans. Several data are available from studies in mouse animal model. Heart-VDR null mice show hypertrophy, while VRD and CYP27B1 null mice are also hypertensive and display increased production of renin, contributing probably of an earlier onset of atherosclerosis (21). Vitamin D may protect against atherosclerosis inhibiting macrophage cholesterol uptake and foam cell formation, and reducing vascular smooth muscle cell proliferation and expression of adhesion molecules in endothelial cells. Recently, elevated level of PTH has emerged as a possible risk factor for CVD since it could promote hypertension development; in addition, hyperparathyroidism could cause heart hypercontractility and calcification of the myocardium. Vitamin D could overcome these processes, promoting for example anti-inflammatory cytokines synthesis (16).

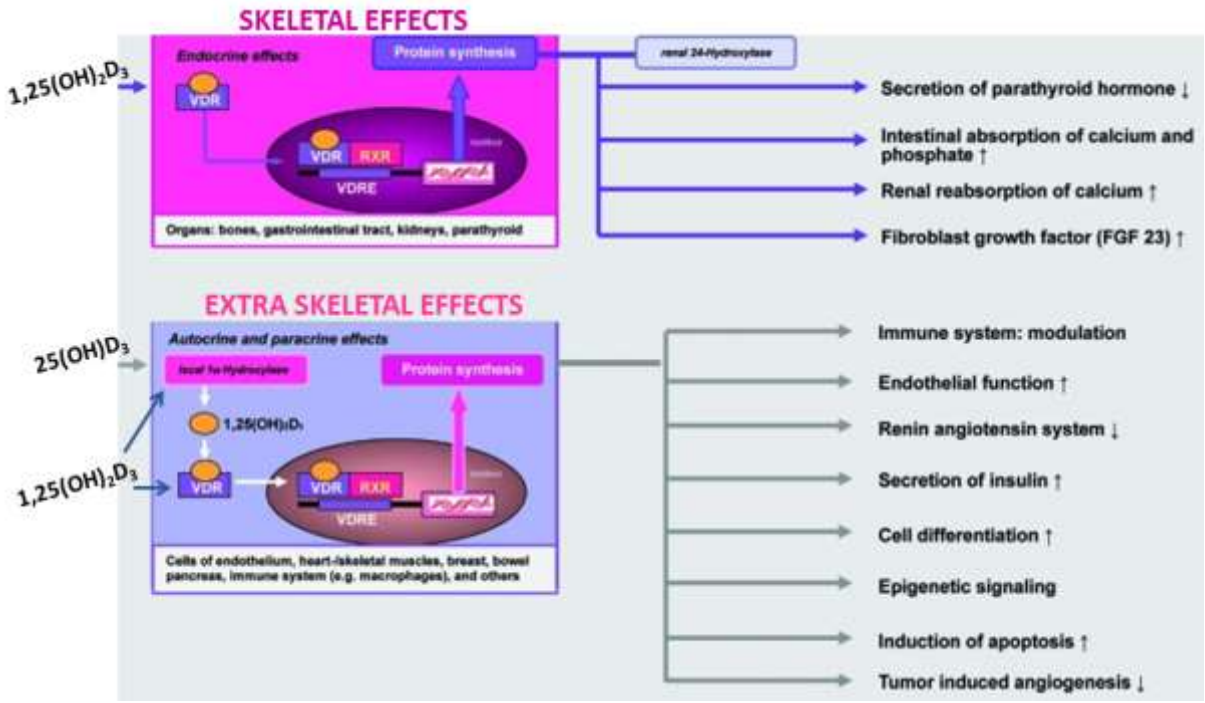

Figure 3. Skeletal and extra skeletal effects of vitamin D. Modified from Gröber U et al. Dermatoendocrinol. 2013.

Other aspects of the vitamin D regulatory network

In a recently published review, Berridge suggests the idea that vitamin D has a crucial activity in keeping the integrity of cell signaling pathways and is called the "custodian of phenotypic stability" (9). The hypothesis supported is that a loss of this integrity could be explained by vitamin D deficiency, representing a risk factor for different diseases. In this custodial role assigned to vitamin D, it may act regulating the expression of the nuclear factor-erythroid-2-related factor 2 (Nrf2) and Klotho, involved in both normal function of reactive oxygen species (ROS) and calcium signaling.

Vitamin D regulates the transcriptional activity of Nrf2, which is a redox-sensitive transcription factor. In normal conditions, Nrf2 activity is repressed and the binding of cullin 3, an ubiquitin ligase, results in Nrf2 degradation in the proteasome. In response to cell stress or ROS increase, Nrf2 is no more associated to repressor molecules and translocates into the nucleus where, binding to antioxidant response elements, activates genes encoding antioxidant and detoxifying enzymes.

Vitamin D controls also Klotho expression, a transmembrane protein implicated in aging and

activated by cleavage with the release of the extracellular portion. Klotho could influence several signaling pathways. It could inhibit insulin/IGF1, upregulating finally antioxidant enzymes such as mitochondrial manganese-superoxide dismutase; it could act as a co-receptor for FGFR, facilitating FGF-23 activity; it could control ion channels activity, like TRPV channels; it could control nitric oxide synthase which generates NO that regulates vasomotor tone. In the animal model of Klotho null mice, they develop, among others defects, premature aging, growth retardation, osteoporosis, cognitive defects, skin atrophy, osteopenia and endothelial dysfunction.

Nrf2 and Klotho, in turn, act on vitamin D regulation; the former increases both VDR and RXR expression, while the latter downregulates 1α-hydroxylase synthesis.

Endothelial cells (ECs)

The endothelium is an active monolayer of endothelial cells located between the vessel lumen and the intimal wall; it composes the inner cellular lining of blood vessel (arteries, veins and capillaries), separating the vascular wall from the circulating blood. It is not only a highly selective barrier but also dynamically regulates blood fluidity, coagulation pathways and vascular tone. It keeps vascular homeostasis by synthesizing and releasing contracting and relaxing factors; vasoconstrictor factors include endothelin-1, angiotensin II, thromboxane A2 and prostaglandin H2, while vasodilation is mediated by several molecules, such as nitric oxide (NO), prostacyclin and endothelium-derived hyperpolarizing factor. NO is the main endogenous vasodilator in the body and could inhibit platelet aggregation, vascular smooth muscle cell proliferation and migration, inflammation, oxidative stress, and leukocyte adhesion. Chronic exposure to cardiovascular risk factors are associated with endothelial dysfunction, that increases oxidative stress, promotes inflammation and reduces NO bioavailability, and could be considered the initial reversible step in the development of atherosclerosis (51-53).

Calcium ions are ubiquitous intracellular second messengers and in the endothelial and smooth muscle cells has a pivotal role in the control of vascular tone. The activity of the ECs, including their ability to synthesize and release vasoactive factors, depends on changes in the intracellular calcium concentration, that can be obtained via calcium entry from the extracellular space or calcium release from the intracellular organelles (52).

Endothelial NO-synthase (eNOS)

Three NO-synthase isoforms could produce NO: NO-synthase I (or neuronal, nNOS, NOS-1) expressed in neurons and skeletal and smooth muscle; NO-synthase II (or inducible, iNOS, NOS-2) in immune cells; and NO-synthase III (or endothelial, eNOS, NOS-3) in cardiomyocytes and platelets and, predominantly, in endothelial cells (52, 54, 55). NOS isoforms generate NO at different rates: eNOS and nNOS produce low concentration of NO, leading to physiological processes regulation, while iNOS generates high NO concentration in response to inflammatory stimuli, such as in activated macrophages, to establish cytotoxic effects and anti-pathogen reactions (56).

eNOS is a Ca^{2+}/calmodulin dependent enzyme and contains an N-terminal oxygenase and a C-terminal reductase domain, linked by a calmodulin binding sequence. It works as homodimer to synthesize NO and L-citrulline from L-arginine and oxygen. In the presence of several cofactors like nicotinamide adenine dinucleotide phosphate (NADPH), flavin adenine dinucleotide (FAD), flavin mononucleotide (FMN), heme, tetrahydrobiopterin (BH_4) and zinc, it catalyzes a five-electron oxidation of one of the guanido nitrogens of L-arginine. Since is a gas, NO then diffuses to the vascular smooth muscle cells and reacts with soluble guanylate cyclase (sGC), leading to cGMP-mediated vasodilatation. In ECs, after enzymatic acylation, myristoylation and reversible palmitoylation, eNOS is predominantly located in the plasma membrane and in the Golgi, associated to caveolin-1 located in caveolae, whose binding inhibits the activity of the enzyme (52, 54). Two mechanisms leading to eNOS activation and involving G protein coupled receptors and heterotrimeric G protein have been identified: intracellular Ca^{2+} mobilization through phospholipase C (PLC) pathway, and phosphatidylinositol-3-kinase (PI3K)/Akt pathway (57, 58). An increase in the intracellular calcium concentration, indeed, is a critical determinant that causes eNOS dissociation from caveolin-1, leading to the activation of the enzyme. Moreover, serine, threonine and tyrosine phosphorylation regulates eNOS activity, either enhancing or suppressing it, depending on the residue and the domain that is involved. Several eNOS agonists such as VEGF, bradykinin and adenosine triphosphate (ATP) promote activating phosphorylation of the enzyme. eNOS expression and activation is also sensitive to shear stress caused by blood flow; low shear stress determines lower NO availability, increasing plaques formation (52, 54).

Nitric oxide (NO)

The discovery of NO as a signaling molecule in the cardiovascular system was awarded in 1998 with the Nobel Prize in Physiology and Medicine (59). NO is now recognized as an endogenous vasodilator and antioxidant, and regulates the vascular endothelium supporting its anticoagulant and anti-thrombogenic capacities, maintaining vascular tone and preventing vascular smooth cell proliferation (60).

NO acts as a signaling molecule by binding to ferrous heme within metalloproteins (such as sGC, cytochrome C oxydase and hemoglobin). The principal mechanism of action of NO is the interaction with the heme group of the sGC in smooth muscle cells adjacent to the endothelium, catalyzing the conversion of guanosine triphosphate (GTP) to cGMP (61). cGMP-dependent protein kinases promote the opening of calcium-dependent potassium channel and determine hyperpolarization of the cell membrane of smooth muscle, thus inhibiting cytosolic calcium influx and promoting cell relaxation and vasodilation. Alternatively, NO could determine molecule modifications. Since it is a highly diffusible molecule with a very short half-life in tissues and physiological fluids (few seconds), it rapidly reacts with superoxide anion (O^{2-}) to form peroxynitrite ($ONOO^-$). $ONOO^-$ oxidizes DNA, proteins, lipids and BH_4, uncoupling eNOS and limiting NO production. It direct influences the dilatory capabilities of the arteries and disrupts NO-induced sGC-mediated signal transduction (62). Nevertheless, NO could be transported by protein carriers or stored locally and cause remote and long-lasting effects in the cardiovascular system (52, 54).

Furthermore, NO signaling depends on its own concentration. Thomas and colleagues demonstrated in MCF7 cells (human breast adenocarcinoma cell line) that NO levels from 10 to 30 nM lead to extracellular signal-regulated kinases (ERK) phosphorylation due to a cGMP-dependent process, mediating proliferative and protective effects (low NO levels, < 1 nM, are sufficient in endothelial cells). When NO concentration is between 30 and 60 nM, Akt phosphorylation occurs, an event that protects against apoptosis, inducing Bad and caspase-9 phosphorylation. Hypoxia-inducible factor-1α (HIF-1α) is stabilized when NO is at greater concentration (about 100 nM) and protects against tissue injury; while at 400 nM, p53 is post-translational modified, resulting in growth arrest or apoptosis. Select signal transduction cascades react accordingly to NO not only in term of concentration but also in term of duration of exposure with different threshold sensitivities, resulting in distinct phenotypic responses. Indeed, HIF-1α is an immediate but transient responder and the protein

disappears when NO concentration falls under the minimal threshold. p53 instead has a delayed response that takes several hours but is sustained long after NO exposure (63).

Reactive oxygen species (ROS)

ROS originate in the mitochondrial electron transport chain (mETC) or are produced by NADPH oxidases (NOX) by an incomplete one-electron reduction of oxygen. Three major ROS exist: superoxide anion (O_2^-), hydrogen peroxide (H_2O_2) and hydroxyl radical (OH). In cellular respiration, most O_2 generates H_2O_2 through enzymes of the superoxide dismutase (SOD) family, comprehending copper-zinc superoxide dismutase (SOD_1 or Cu, Zn-SOD) present in the intermembrane space and in the cytosol, manganese superoxide dismutase (SOD_2 or Mn-SOD) present in the mitochondria matrix, and SOD_3 present in the extracellular matrix. Hydrogen peroxide could subsequently be converted to hydroxyl radical by ferrous or copper iron, or a final reducing step could convert it to water by catalase, glutathione peroxidase and peroxiredoxin III activity. In ECs, ROS into the cytosol could stimulate further ROS production by NOX_2 through redox-sensing protein kinase C (PKC) isoforms and Src family kinases activation (64, 65).

While ROS are product of normal mitochondrial metabolism, oxidative stress occurs when an imbalance arises between ROS production and antioxidant capacity, through excess ROS production and/or antioxidant depletion. ROS can adversely alter lipids (causing their peroxidation), proteins (determining the loss of the enzyme activity) and DNA (resulting in mutagenesis and carcinogenesis), and have been implicated in aging and a number of human diseases, such as cancers, neurodegenerative and cardiovascular diseases. It is also well known that ROS can regulate apoptosis and autophagy pathways (65-67).

Endothelial dysfunction

Endothelial dysfunction should be considered as endothelial activation from a quiescent phenotype and it is identified as an initial step in the development of CVD, characterized by reduced NO bioavailability that predisposes to vasoconstriction and thrombosis (68). Several factors can contribute to this process, such as decreased eNOS expression, presence of eNOS antagonist, low L-arginine or BH_4 concentration, increased NO degradation or ROS production, exposure to inflammatory cytokines and growth factors (62). Indeed, the

fundamental change is a switch in the signaling from an NO-mediated silencing of cellular processes toward activation by redox signals. The generation of hydrogen peroxide, which could react with cysteine groups in proteins, alters their function, determining transcriptional factors phosphorylation, induction of nuclear chromatin remodeling and protease activation. eNOS, normally involved in the maintenance of the quiescent state of the endothelium, could be uncoupled causing superoxide formation if the key cofactor tetrahydrobiopterin is not present, or hydrogen peroxide production if the substrate L-arginine is deficient. The mitochondria are a source of ROS during hypoxia or conditions of increased substrate delivery, such as in obesity-related metabolic disorders or type II diabetes, which are characterized by hyperglycemia and increased circulating free fatty acids. The interaction between ROS and NO results in further endothelial activation and inflammation. (69).

MATERIALS AND METHODS

Endothelial cell cultures

Porcine aortic endothelial (PAE) cells were grown in Dulbecco's Modified Eagle Medium (DMEM) supplemented with 10% heat inactivated fetal bovine serum (FBS), penicillin (100 U/ml), streptomycin (100 mg/ml) and L-glutamine (2 mM) at 37°C in a humidified atmosphere containing 5% CO_2. All the reagents were from Euroclone, Milan, Italy.
Human umbilical vein endothelial cells (HUVECs) were isolated from 25 human umbilical vein cord as previously described (70, 71). HUVECs were cultured in 0.1% gelatin-coated flask with Endothelial Growth Medium-2 (EGM-2) containing 2% FBS, 0.04% hydrocortisone, 0.4% hFGF-B, 0.1% VEGF, 0.1% R3-IGF-1, 0.1% ascorbic acid, 0.1% hEGF, 0.1% GA-1000, 0.1% heparin (complete medium; all from Lonza, Walkersville, MD, USA) and maintained at 37°C and 5% CO_2. For all experiments cells were used from passage 3 to passage 6.

Cell treatments

Cells were treated with different concentrations of the biologically active form of vitamin D (1-10-100 nM; 1α,25-dyhydroxyvitamin D3, catalog number D1530, Sigma Aldrich, St. Louis, MO, USA) dissolved in ethanol. In all the experiments of this work, the treatment with vitamin D refers to its biologically active form.
To evaluate NO synthesis involvement in both PAE cells and HUVECs proliferation and migration following vitamin D treatment, some experiments were performed in the presence of the eNOS inhibitor Nω-Nitro-L-arginine methyl ester hydrochloride (L-NAME; Sigma Aldrich). L-NAME was dissolved in serum free medium and used at a final concentration of 10 mM for PAE cells (70) and 1 mM for HUVECs (72, 73), as reported in literature.
Some experiments were also performed in the presence of the synthetic VDR antagonist ZK159222 or the specific VDR ligand chemically synthesized ZK191784 (both from Bayer Pharma AG, Berlin, Germany), alone or in combination with vitamin D, in order to verify the effective VDR involvement in the pathway of interest.

The oxidative stress condition was induced in HUVEC cultures using H_2O_2. The administration of exogenous H_2O_2 is a widely used method to reproduce a cellular damage similar to what occurs in myocardial ischemia/reperfusion injury (65).

Cell viability (MTT assay)

10^5 HUVEC were plated in gelatin-coated 24 well plates in complete medium and, after adhesion, cells were incubated for 4-6 hours in DMEM without red phenol and FBS, and supplemented with 2 mM glutamine and 1% penicillin-streptomycin (starvation medium; all from Sigma Aldrich). After vitamin D treatments, cell viability was determined using the "In Vitro Toxicology Assay Kit", 3-(4,5-dimethylthiazol-2-yl)-2,5-diphenyltetrazolium bromide based (MTT, Sigma Aldrich), following manufacturer's instructions. Cell viability was calculated comparing treatments to control cells, considered as 100% viable. Briefly, cells were incubated with 1% MTT dye dissolved in starvation medium for 2 h at 37°C in incubator. Then, the medium was removed and the purple formazan crystals formed during the reaction were dissolved in equal volume of MTT Solubilization Solution to the original culture medium. Cell viability was determined by measuring the absorbance through a spectrometer (BS 1000 Spectra Count) at 570 nm with correction at 690 nm.

Cell proliferation

$2.5x10^5$ PAE cells were seeded on Petri dishes and let adhere for 5 hours. Non adherent cells were removed by washes in phosphate buffered saline (PBS) and complete medium was replaced with low FBS medium (1%) without phenol red for 24 hours.
10^3 HUVECs were plated in gelatin-coated 96 well plate and let adhere; then complete medium was replaced with low FBS medium (0.2%) without phenol red.
For both cell types, proliferation has been evaluated in low serum conditions to synchronize cell culture. After vitamin D treatments, cells were fixed in 3.7% formaldehyde-3% sucrose solution, stained with 1% toluidine blue solution and photographed at 10X magnification using an optical microscope (Leica ICC50HD). Cell proliferation was evaluated by counting cells in 10 random fields in 3 different samples of at least 3 different experiments. Results were expressed as cells/mm^2 ± standard deviation (S.D.).

NO production (Griess assay)

10^3 PAE cells were seeded in 96 well plate and $5x10^5$ HUVECs were plated in gelatin-coated 24 well plate, let adhere and put in low FBS medium without phenol red. After vitamin D treatments, for both cell types, NO production was detected in culture supernatants in which an equal volume of Griess reagent (Promega, Madison, WI, USA) was added, following manufacturer's instructions. After 10 min of incubation the absorbance of supernatants was measured by means of a spectrometer (BS1000 Spectra Count). Results were expressed as percentage (%) compared with control values.

Three-dimensional matrix migration assay

PAE cells and HUVECs were seeded in 12 wells plates and grown in complete medium to reach a ~70% confluent monolayer. The 3D hydrogel matrix used was Epigel B, an anionic hydrogel composed of gelatin and polyglutamic acid (without added growth factor, Epinova Biotech, Novara, Italy). The 3D matrix were lean onto cell monolayers in 250 µl of complete cell culture medium containing different amounts of vitamin D, and cell migration was monitored daily by optical microscopy. After 3 days, cell culture medium was replaced with fresh medium. After 7 days, hydrogel samples were fixed in 3.7% formaldehyde-3% sucrose solution, stained with 2 µg/ml of Hoechst 33342 solution (Sigma Aldrich) in order to stain cell nuclei and then transferred onto glass microscope slides before observation under UV light using a Leica DM500 fluorescence microscope. Cell migration was evaluated by counting migrated cells into 3D matrix. For each experimental condition, 3 samples were analyzed at 10X magnification, selecting 10 random fields and results were expressed as no. cells/HPF (high power microscope field) ± S.D.

Gelatin zymography

In order to detect gelatinolytic activity, conditioned media from cells migrated into the 3D matrix for 7 days were separated by electrophoresis on SDS-polyacrylamide gels containing 0.2% gelatin. Briefly, samples were loaded onto zymograms without denaturation. After running, gels were washed at room temperature (RT) for 2 h in 2.5% Triton X-100 solution and incubated overnight at 37°C in 0.5 M TrisHCl, 0.2 M NaCl, 5 mM CaCl2, 1 mM ZnCl2

buffer. Gels were then fixed in MetOH/Acetic Acid (50:10) solution and stained in 0.5% Coomassie Blue in MetOH/Acetic Acid (40:10) solution. Images of stained gels were acquired after appropriate destaining. Gelatinolytic activity was detected as white bands on a dark blue background and quantified by densitometric analysis using ImageJ software.

Reverse transcription-polymerase chain reaction (RT-PCR)

To detect changes in gene expression after stimulations, total RNA was extracted from control and treated samples using Ribozol (Amresco, Solon, OH, USA) according to the manufacturer's instructions. RNA integrity was assessed using Nanodrop (Thermo Fisher Scientific, Wilmington, DE, USA). Single-strand cDNA was synthesized from 300 ng of total RNA using High Capacity cDNA Reverse Transcription kit (Applied Biosystems, Foster City, CA, USA) according to manufacturer's instructions. cDNA products were used as templates for PCR amplification in an automated thermal cycler (Technegene DNA Thermal Cycler, Techne, UK). The oligonucleotide primers used are reported in Table 2. RT-PCR runs were performed with an initial activation step of 4 min at 94°C followed by 35 routine cycles, as follow: incubation at 94°C for 30 sec, 68°C for 30 sec and 72°C for 1 min. One additional cycle of 72°C for 7 min was run to allow trimming of incomplete polymerization. Control reactions were performed in the absence of cDNA. Amplified PCR products were separated on 1.8% agarose gel containing ethidium bromide and visualized by UV illumination. Images of stained gels were acquired and the levels of MMP-2 and β-actin PCR products were quantified by densitometric analysis using ImageJ software. Data were expressed as MMP-2/β-actin ratio.

	Primer forward	Primer reverse
MMP-2	5' - TAC AAA GGG ATT GCC AGG AC - 3'	5' - GGC AGC CAT AGA AGG TGT TC - 3'
β-actin	5' - ACA CTG TGC CCA TCT ACG AGG GG - 3'	5' - ATG ATG GAG TTG AAG GTA GTT TCG TGG AT - 3'

Table 2. MMP-2 and β-actin primers used in RT-PCR.

ROS production

The rate of superoxide anion release was used to examine vitamin D effects against oxidative stress. The superoxide anion production was measured as superoxide dismutase-inhibitable reduction of cytochrome C. 100 µl of cytochrome C were added in all samples, and in another one, 100 µl of superoxide dismutase was added for 30 min in an incubator (all substances from Sigma Aldrich). The absorbance changes in the supernatants were measured at 550 nm using Wallac Victor model 1421 spectrometer (PerkinElmer). O^{2-} was expressed as nanomoles per reduced cytochrome C per microgram of protein, using an extinction coefficient of 21000 ml/cm, after the interference absorbance subtraction (74).

Measurement of mitochondrial permeability transition pore (MPTP)

In order to measure MPTP, after each stimulation and in the other sample pretreated with l µM cyclosporin A for 30 min (75), the medium was removed and the sarcolemmal membrane was permeabilized with 10 µM digitonin (76) for 60 sec in an intracellular solution buffer (135 mM KCl, 10 mM NaCl, 20 mM hepes, 5 mM pyruvate, 2 mM glutamate, 2 mM malate, 0.5 mM KH2PO4, 0.5 mM MgC12, 15 mM 2,3-butanedionemonoxime, 5 mM EGTA, 1.86 mM CaC12; all substances from Sigma Aldrich) and then loaded with 5 µM calcein/acetomethoxy derivate of calcein for 40 min at 37°C. Cells were then washed with Tyrode's solution for 10 min, and the fluorescence was measured by Wallac Victor model 1421 spectrometer at fluorescence excitation and emission of 488 and 510 nm, respectively.

Membrane potential assay

After each stimulation, the medium was removed and the cells were incubated with 5,5',6,6'-tetrachloro-1,1',3,3'-tetraethylbenzimidazolylcarbocyanine iodide 1X diluted in Assay Buffer 1X for 15 min at 37°C following the manufacturer's instruction (APO-LOGIX JC-1; Bachem, San Carlos, CA, USA). After the incubation, the cells were washed twice with Assay Buffer lX and then the suspensions were transferred in triplicates to a black 96 well plates. The red (excitation 550 nm/emission 600 nm) and green (excitation 485 nm/emission 535 nm) fluorescence were measured using Wallac Victor model 1421 spectrometer, and the rate of apoptotic cells was obtained by determining the ratio of red to green fluorescence (77).

Western blot analysis

To evaluate protein expression, HUVECs were stimulated and then washed with iced-PBS 1X supplemented with 2 mM sodium orthovanadate and lysed in an iced Ripa buffer (50 mM hepes, 150 mM NaCl, 0.1% SDS, 1% Triton-X 100, 1% sodium deoxycholate, 10% glycerol, 1.5 mM MgCl2, 1mM EGTA, 1mM NaF) supplemented with 2 mM sodium orthovanadate and 1:100 protease inhibitor cocktail. The protein extract was quantified by using bicinchoninic acid protein assay (BCA, Thermo Scientific, Massachusstes, USA) and 40 µg of each sample was dissolved in Laemmli buffer 5X, heated at 95°C for 5 min, resolved on 8 % or 15 % SDS PAGE gels and transferred to a polyvinylidene fluoride membrane. The membranes were incubated overnight at 4°C in agitation with specific primary antibodies: anti-Bax (0.5 µg/ml; Calbiochem), anti-Beclin 1 (0.4 µg/ml; Santa-Cruz), anti-caspase-3 (0.4 µg/ml; Santa-Cruz), anti-cytochrome C (1 µg/ml; Sigma Aldrich), anti-caspase-8 (5 µg/ml; Sigma Aldrich), anti-caspase-9 (3 µg/ml; Sigma Aldrich), and anti-Ki67 (3 µg/ml; Sigma Aldrich); anti-phospho-p44/42 MAP kinase (Thr202/Tyr204 1:1000; Cell Signaling), anti-ERK1/2 (1:1000; Cell Signaling), anti-phospho-Akt (Ser473 1:1000; Cell Signaling) and anti-Akt (1:1000; Cell Signaling), anti-β-actin (1:5000; Sigma Aldrich). The membranes were washed and then incubated with horseradish peroxidase-coupled goat anti-rabbit Ig and anti-mouse Ig and were developed by use of a non-radioactive method through Western Lightning chemiluminescence. Densitometric analysis was performed using Quantity One image analysis software (BioRad). The quantification of protein expression was normalized to specific total protein, which was loaded on each respective blot, and to β-actin detection, and was expressed as a percentage.

Caspase-3 activity

For the assay, 50 µl of each sample were added into 75 µl of Caspase-3 Colorimetric Substrate in 96 well plate ready to use. In addition, 50 µl of Caspase-3 Enzyme Standard (1000 U/m1-62.5 U/m1) into 75 µl of Caspase-3 Colorimetric Substrate and 125 µl of p-nitroaniline (Calibrator Optical Density) were tested. The reaction was allowed to warm up to 37°C and maintained for 3 h and then measured by a spectrometer (Wallac Victor model 1421) at 405 nm following the manufacturer's instruction (Assay Designs Temaricerca,

Bologna, Italy). The results were obtained by interpolation as means Activity Unit/ml and expressed as percentage.

Immunocytochemistry

HUVECs were plated on 4 well chamber slides (Thermo Scientific) and immunostained with Annexin V (13 μg/ml; Sigma Aldrich) and Beclin 1 (4 μg/ml; Santa Cruz Biotechnology) antibodies. Briefly, after the stimulations, the cells were fixed using iced-buffer PAF (3.7 % formaldehyde and 1 % sucrose in PBS 1X) for 20 min, washed 3 times with iced-PBS 1X and then permeabilized with iced-0.5% Triton X-100 in PBS 1X for 20 min at 4°C. Endogenous peroxidase activity was quenched during 8 min of incubation with 3% H_2O_2 in PBS 1X, and then blocked with 3% BSA in PBS 1X for 1 h. Slides were incubated overnight at 4°C with specific primary antibody diluted in PBS 1X and then incubated with the biotinylated secondary antibody for 20 min. Slides were then washed in PBS 1X, incubated for 20 min with streptavidin solution (Vectastain® R.T.U. ABC Reagent, D.B.A. Italia s.r.l., Milan, Italy) and developed with 3-3'diaminobenzidine (DAB, Dako Italia Spa, Milan Italy), then rinsed, counterstained with Mayer's hematoxylin and mounted with aqueous mounting medium. Finally, cells were visualized using a light microscope (Leica, Germany).

Immunofluorescence

HUVECs were plated on chamber slides and stained with caspase-3 antibody (13 μg/ml; Santa Cruz). Briefly, after the stimulations, the cells were fixed using iced-buffer PAF, washed 3 times and then permeabilized as previously described. The slides were then incubated in block solution (1% BSA and 5% FBS in PBS 1X) for 30 min at RT and incubated with specific primary antibody diluted in PBS 1X overnight at 4°C. The slides were then incubated with fitch-secondary antibodies (5 μg/ml; Sigma Aldrich) diluted in PBS 1X for 1 h in the dark, counterstained with DAPI (1 μg/ml; Sigma Aldrich) diluted in PBS 1X for 5 min in the dark at RT and finally mounted using Vectashield (D.B.A. Italy). Cells were visualized using a fluorescence microscope (Leica DM500).

TUNEL assay

For the detection of the endonucleolytic cleavage of chromatin, characteristic of apoptosis, HUVECs were plated on chamber slides and analyzed using a TUNEL assay kit (ApopTag Plus Peroxidase Apoptosis Detection Kit, Merck Millipore, Milan, Italy). Briefly, after the stimulations, the cells were fixed, washed and permeabilized, and the endogenous peroxidase activity was quenched as described in the Immunocytochemistry section. Then the slides were processed with TUNEL kit following the manufacturer's instructions, counterstained with Methyl Green Solution and mounted with aqueous mounting medium. Nuclear morphological changes were visualized using light microscope (Leica, Germany).

Statistical analysis

Results are expressed as means ± S.D. of at least 3 independent experiments for each protocol. One-way Anova followed by Bonferroni post-test was used for statistical analysis. Probability values of $p<0.05$ was considered as statistically significant.

RESULTS

During my PhD fellowship I focused my researches predominantly on the extra skeletal effects of vitamin D and below I present the results obtained, which have been published in three articles on international scientific journals.

Vitamin D effects on NO production in physiological condition and during oxidative stress

NO production was evaluated using Griess method both in physiological condition and during oxidative stress.

As shown in Figure 4, NO accumulation in PAE cells in physiological condition increases after 1 nM (18.03 ± 5.13 %), 10 nM (18.67± 0.83 %) and 100 nM (25.11± 4.91 %) vitamin D stimulation compared with basal values.

To verify whether vitamin D effect on NO production was mediated by VDR, PAE cells were treated with vitamin D in combination with the specific synthetic VDR antagonist ZK159222. This stimulation almost completely inhibits vitamin D-induced NO production (Figure 4), reducing NO levels to basal.

To analyze the vitamin D effects on NO production induced by oxidative stress, HUVECs were treated with H_2O_2, vitamin D, and/or the synthetic VDR agonist ZK191784. 1 nM vitamin D alone is able to cause NO release ($p<0.05$) of approximately 70.33 ± 4.73 % compared with controls, and this effect is amplified ($p<0.05$) in the sample treated with vitamin D in combination with 1 nM ZK191784 (123.3 ± 6.51 %; Figure 5). These data confirmed what was observed in a previous study of our laboratory on NO production caused by vitamin D in ECs (70). Oxidative stress induced by 200 μM H_2O_2 causes a reduction in NO release of about 10 ± 1.52 % ($p<0.05$) compared with controls, which is significantly reversed in the samples pretreated with 1 nM vitamin D alone (26.33 ± 4.16 %; $p<0.05$) and amplified in combination with 1 nM ZK191784 (53.33 ± 7.64 %). In the samples treated first with H_2O_2, the subsequent stimulation with vitamin D alone or in combination with ZK191784 is not able to counteract the negative effects caused by the oxidative stress event on NO production (Figure 5). These results suggest that vitamin D is able to counteract the negative effects induced by oxidative stress and confirm the ability of vitamin D to induce NO release.

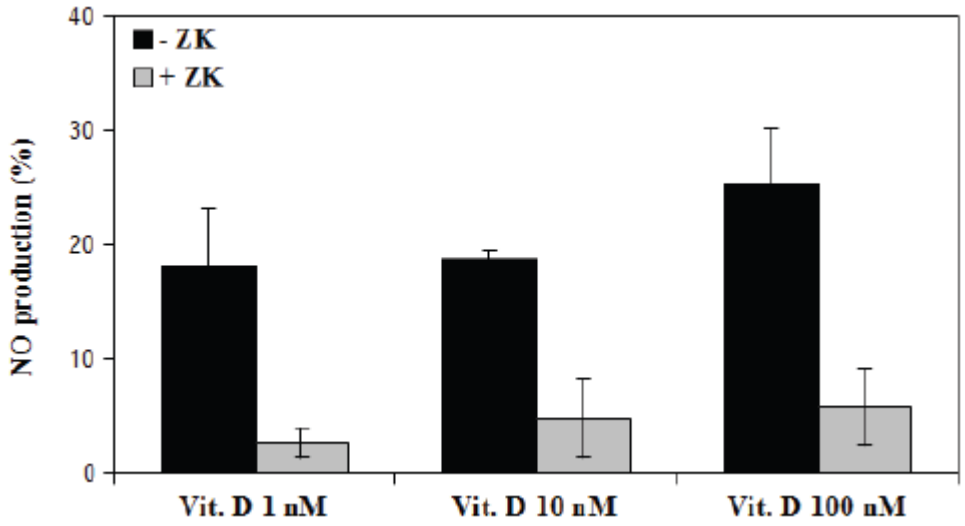

Figure 4. NO production. Quantification of NO production measured by means of Griess method and expressed as percentage of control values. NO production was evaluated in the presence of different vitamin D concentrations (1-10-100 nM). Black bars = cells without ZK159222 addition; grey bars = cells + ZK159222.

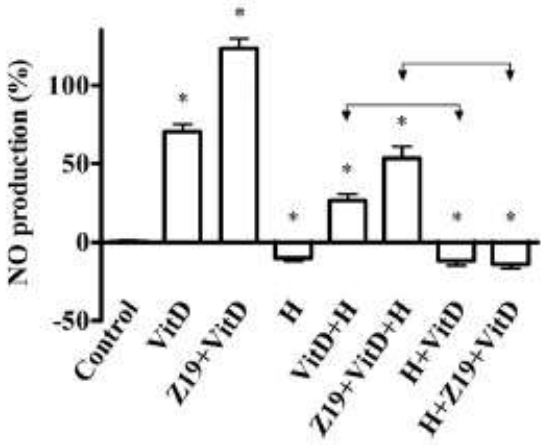

*Figure 5. Effects on NO production determined by means of the Griess method, induced by vitamin D (VitD; 1 nM) alone or in combination with ZK191784 (Z19; same concentration) and/or H_2O_2 (H; 200 μM) in HUVEC cultures. C=control; Z19+VitD, VitD+H, Z19+VitD+H, H+VitD, H+Z19+VitD=combination. * $p<0.05$ vs control; arrows indicate H+VitD $p<0.05$ vs VitD+H and H+Z19+VitD $p<0.05$ vs Z19+VitD+ H. Data are means (%) ± S.D. of 5 independent experiments.*

Vitamin D induces endothelial cells proliferation through a NO-dependent pathway

Cells proliferation has been evaluated in low serum conditions to synchronize cell culture after 24 or 48 h in starvation medium for PAE cells and HUVECs respectively in the presence or absence of vitamin D (1-10-100 nM). As shown in Figures 6 and 7, vitamin D induces a significant dose-dependent increase in cells growth at all concentrations tested. The maximal effect is reached stimulating PAE cells with 10 nM vitamin D, while at the highest concentration tested (100 nM) vitamin D effect on cell proliferation is less potent ($p<0.05$; Figures 6A and 6B). The observed cellular density is almost doubled compared with control samples for PAE cells (690 ± 210 cells/mm^2 vs 354 ± 84 cells/mm^2, $p<0.01$) and HUVECs (Figure 7A). Ethanol used as vehicle for vitamin D administration does not affect cell proliferation (data not shown).

In order to evaluate NO involvement in the observed vitamin D-induced effects, proliferation assays were also performed in the presence of L-NAME, the arginine analog inhibiting NO synthesis. In these conditions, vitamin D is no more able to induce cell proliferation, as shown in Figures 6A and 6B for PAE cells, and 7A and 7C for HUVECs, respectively. L-NAME presence does not alter control cells proliferation, while completely reverts vitamin D-induced cell proliferation.

The stimulation of HUVECs with the VDR ligand ZK159222 causes a significant decrease in vitamin D-induced cell proliferation, confirming the role of VDR in the effects mediated by vitamin D (Figures 7A and 7B).

Moreover, some HUVEC samples treated as described above were fixed at 24 h and photographed for morphological analysis. Noteworthy, an increase in cell mitosis has been observed only in vitamin D-treated specimens and not in samples with L-NAME (Figure 8).

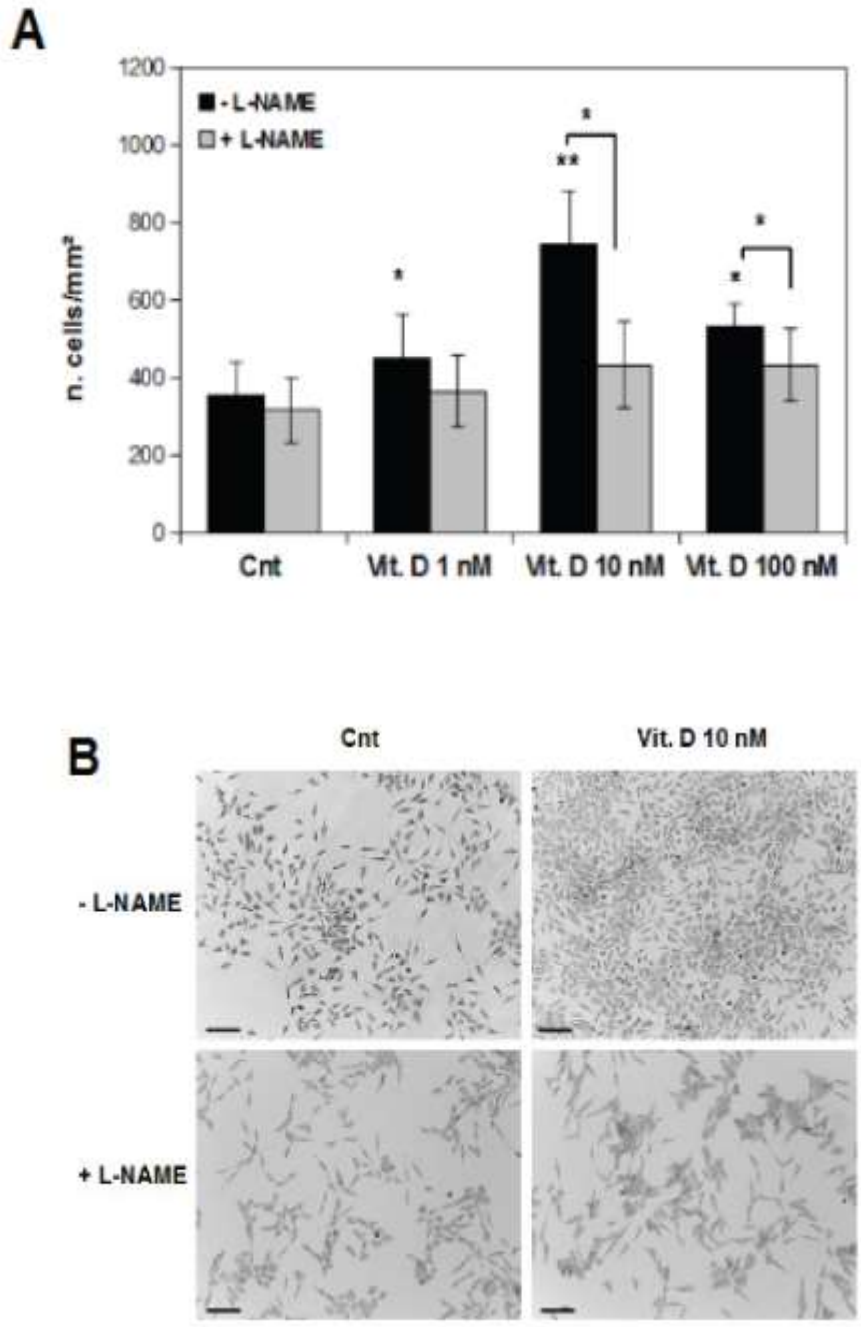

*Figure 6. PAE cells proliferation. A) Determination of PAE cells proliferation in the presence of different concentrations of vitamin D (1-10-100 nM) after 24 h of incubation. Results are expressed as n. cells/mm^2 ± S.D. Black bars = cells without L-NAME addition; grey bars = cells + L-NAME. * p<0.05; ** p<0.001. B) Optical microscopy images of control and vitamin D (10 nM)-treated cells both in absence or presence of L-NAME after 24 h of incubation, stained with toluidine blue. Magnification = 10X. Scale bar = 150 μm.*

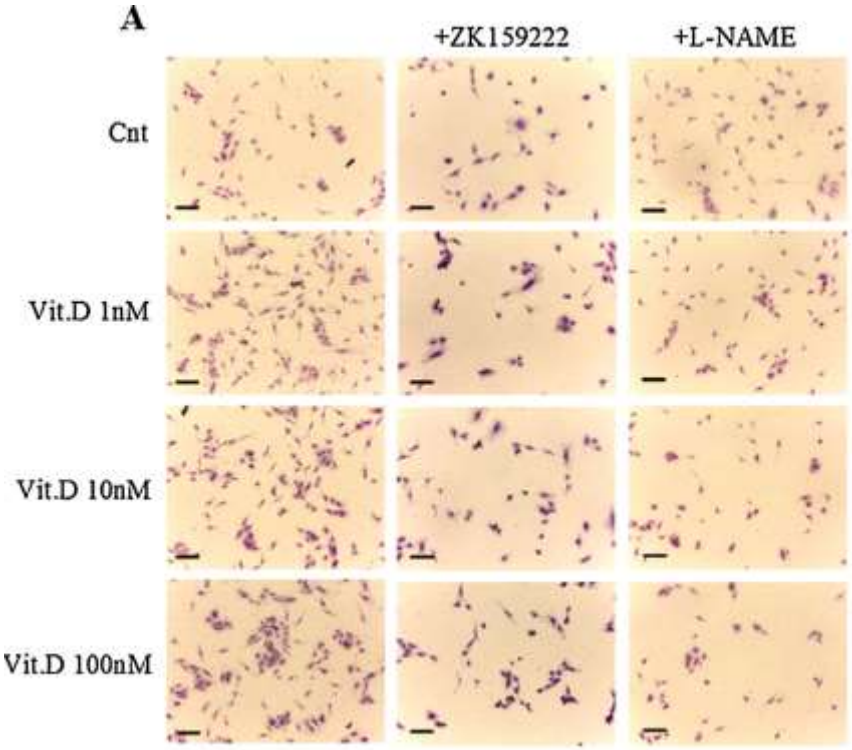
A
+ZK159222
+L-NAME
Cnt
Vit.D 1nM
Vit.D 10nM
Vit.D 100nM

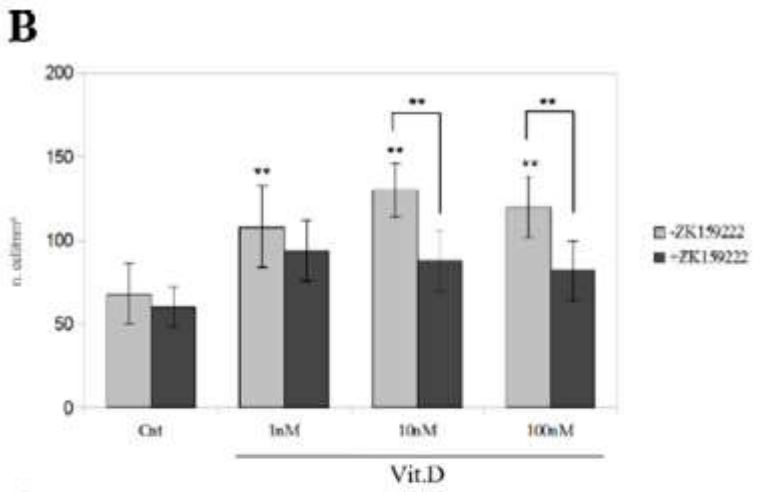
B
200
150
100
50
0
Cnt
1nM
10nM
100nM
Vit.D
-ZK159222
+ZK159222

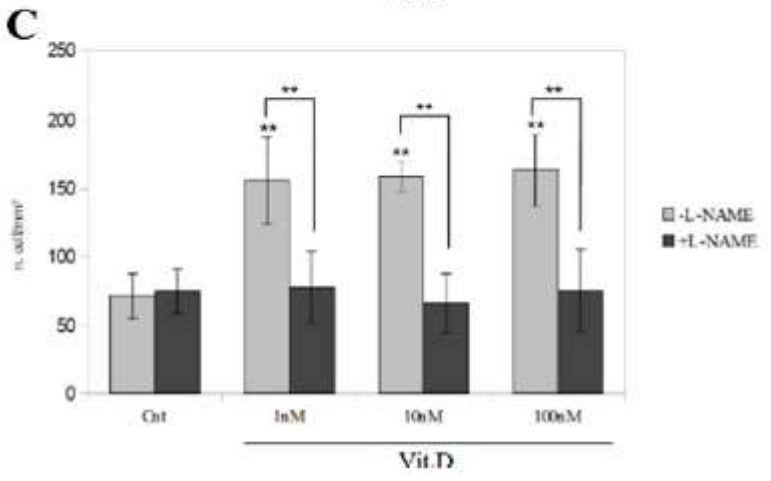
C
250
200
150
100
50
0
Cnt
1nM
10nM
100nM
Vit.D
-L-NAME
+L-NAME

*Figure 7. HUVECs proliferation. (A) Optical microscopy images of control and vitamin D (1–10-100 nM) treated cells both in absence or presence of ZK159222 and L-NAME after 48 h of incubation, stained with toluidine blue. Original magnification = 10X. Scale bar = 125μm. (B) Determination of HUVECs proliferation in the presence of different vitamin D concentration (1–10-100 nM) and ZK159222 co-stimulation after 48 h of incubation. Results are expressed as n. cells/mm^2 ± S.D. Grey bars = cells without ZK159222 addition; black bars = cells + ZK159222. One-way ANOVA followed by Bonferroni post-test were used for statistical analysis. ZK = ZK159222. **p < 0.01. (C) Determination of HUVECs proliferation in the presence of different vitamin D concentration (1–10-100 nM) and L-NAME after 48 h of incubation. Results are expressed as n. cells/mm^2 ± S.D. Grey bars = cells without L-NAME addition; black bars = cells + L-NAME. One-way ANOVA followed by Bonferroni post-test were used for statistical analysis. **p < 0.01.*

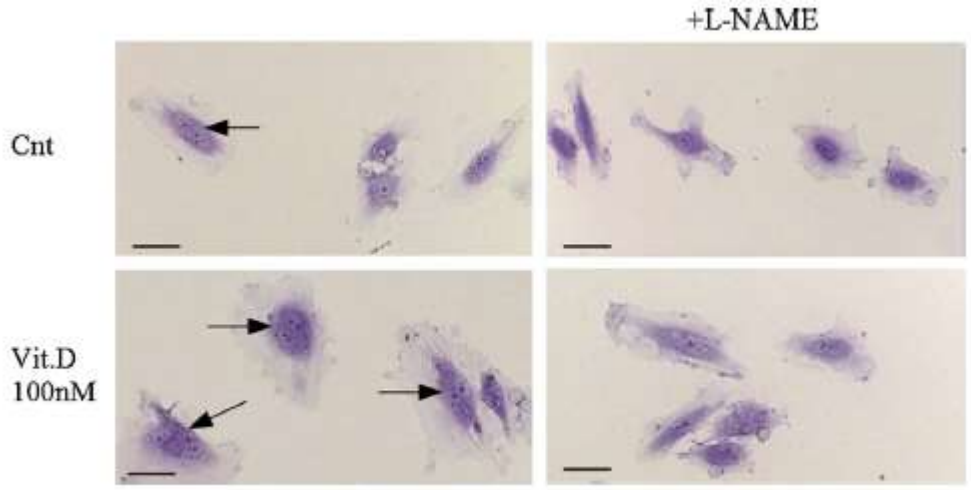

Figure 8. Cell mitosis. Representative optical images of control and vitamin D-treated cells both in absence or presence of L-NAME after 24 h of incubation, stained with crystal violet. Original magnification = 20X. Scale bar = 15 μm.

Vitamin D induces endothelial cell migration in a 3D matrix through a NO-dependent pathway

Cell migration has been evaluated in a three-dimensional model. The 3D matrix used in these experiments was an anionic hydrogel made of gelatin and polyglutamic acid, which has previously been described as a good substrate for cell growth (78, 79) and was lean on 70% confluent cell monolayers.

As shown in Figures 9A and 10, PAE cells migration evaluated counting the cells migrated in the 3D matrix for 7 days increases significantly only in presence of 100 nM vitamin D ($p<0.05$). HUVECs migration increases significantly only in the presence of 10 nM and 100 nM Vit. D ($p<0.05$ and $p<0.01$ respectively; Figures 11A and 11B).

In order to evaluate NO involvement in the observed phenomenon, the same experiments were also performed stimulating cells with L-NAME in the presence or absence of the most effective vitamin D concentration. L-NAME treatment do not affect control cells migration, while it significantly reduces vitamin D-induced hydrogel invasion ($p<0.05$ compared with vitamin D alone for PAE cells; Figures 9B and 10. $p<0.01$ compared with vitamin D alone for HUVECs; Figures 12A and 12B).

To demonstrate the relevance of VDR on these effects, some experiments were also performed in cultured HUVECs with vitamin D alone or in co-stimulation with ZK159222. This VDR ligand reduces vitamin D-induced migratory effect, as shown in Figure 13.

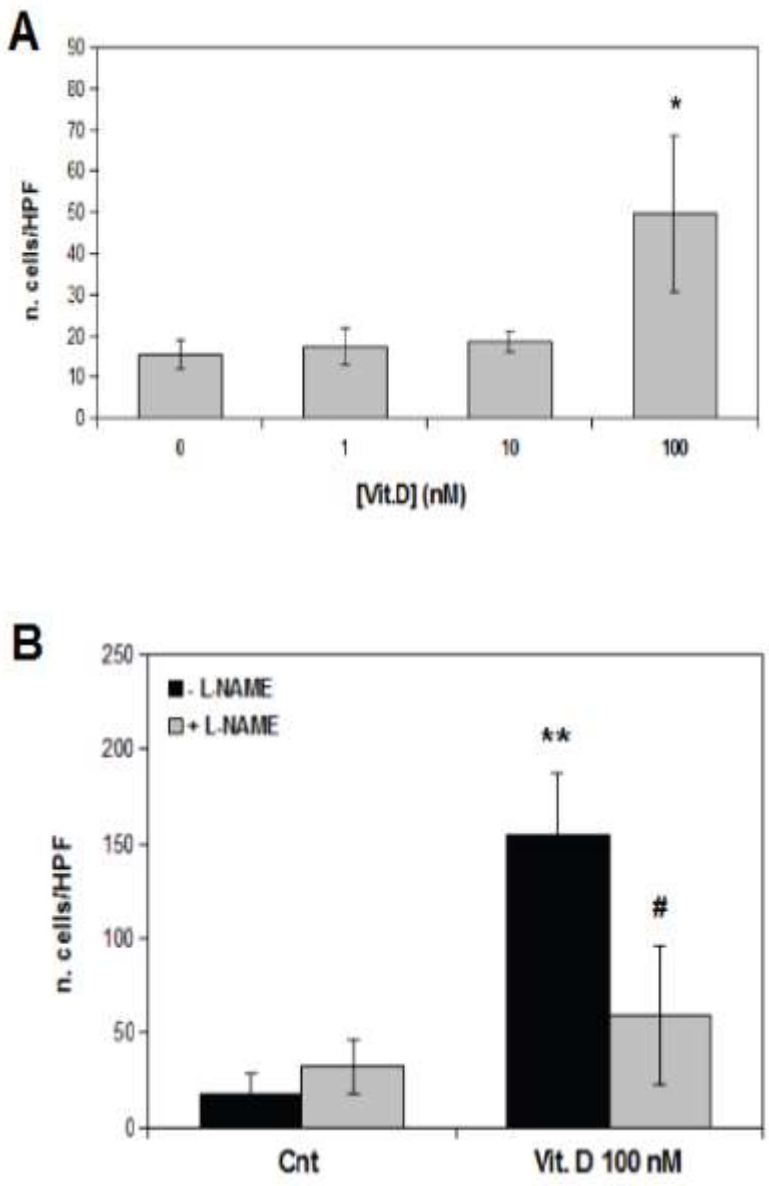

*Figure 9. PAE cells migration into a 3D matrix. A) Determination of PAE cells migration after 7 days of incubation in the presence of different vitamin D concentrations (1-10-100 nM). Results are expressed as n. cells/HPF ± S.D. * p<0.05. B) Determination of control and vitamin D (100 nM)-treated cells migration both in the presence or absence of L-NAME after 7 days of incubation. *p<0.01 compared with control sample; # p<0.05 compared with VitD 100 nM alone.*

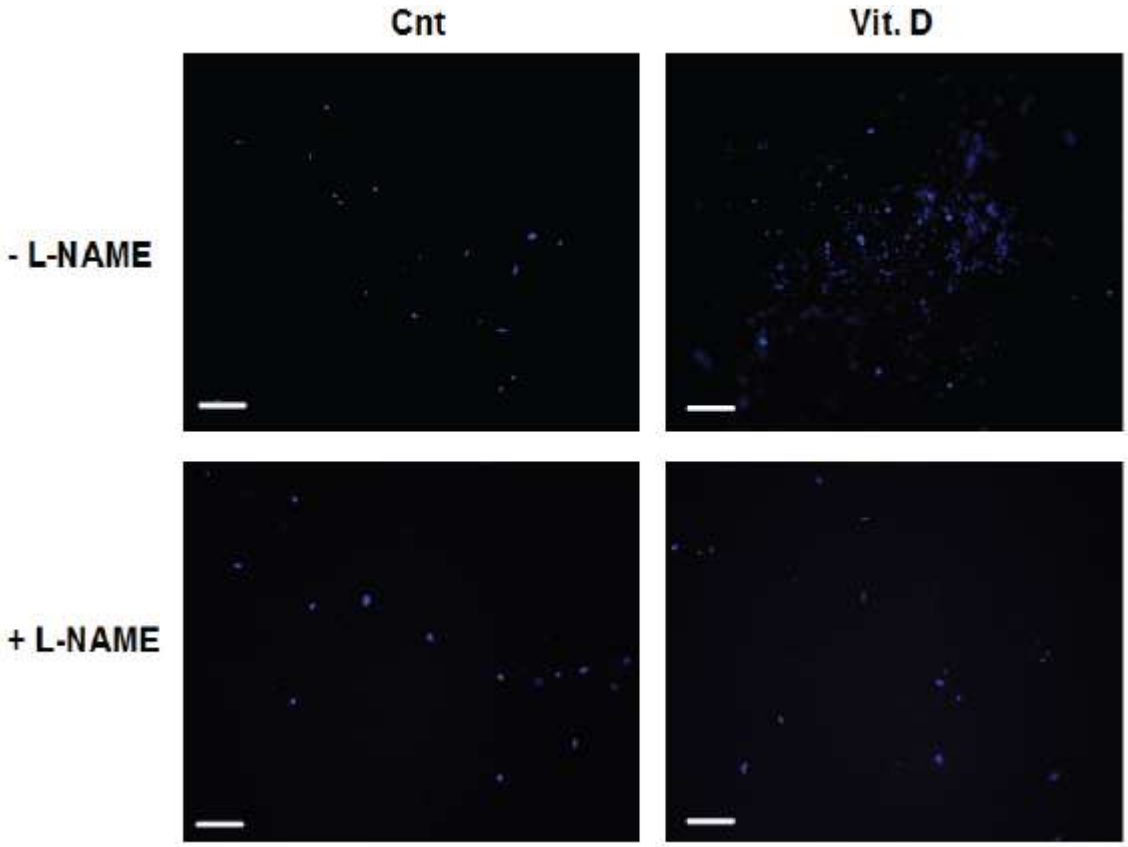

Figure 10. Optical microscopy images of control and vitamin D (100 nM)-treated cells both in the presence or absence of L-NAME after 7 days of incubation, stained with Hoechst 33342. Magnification = 10X. Scale bar = 60 μm.

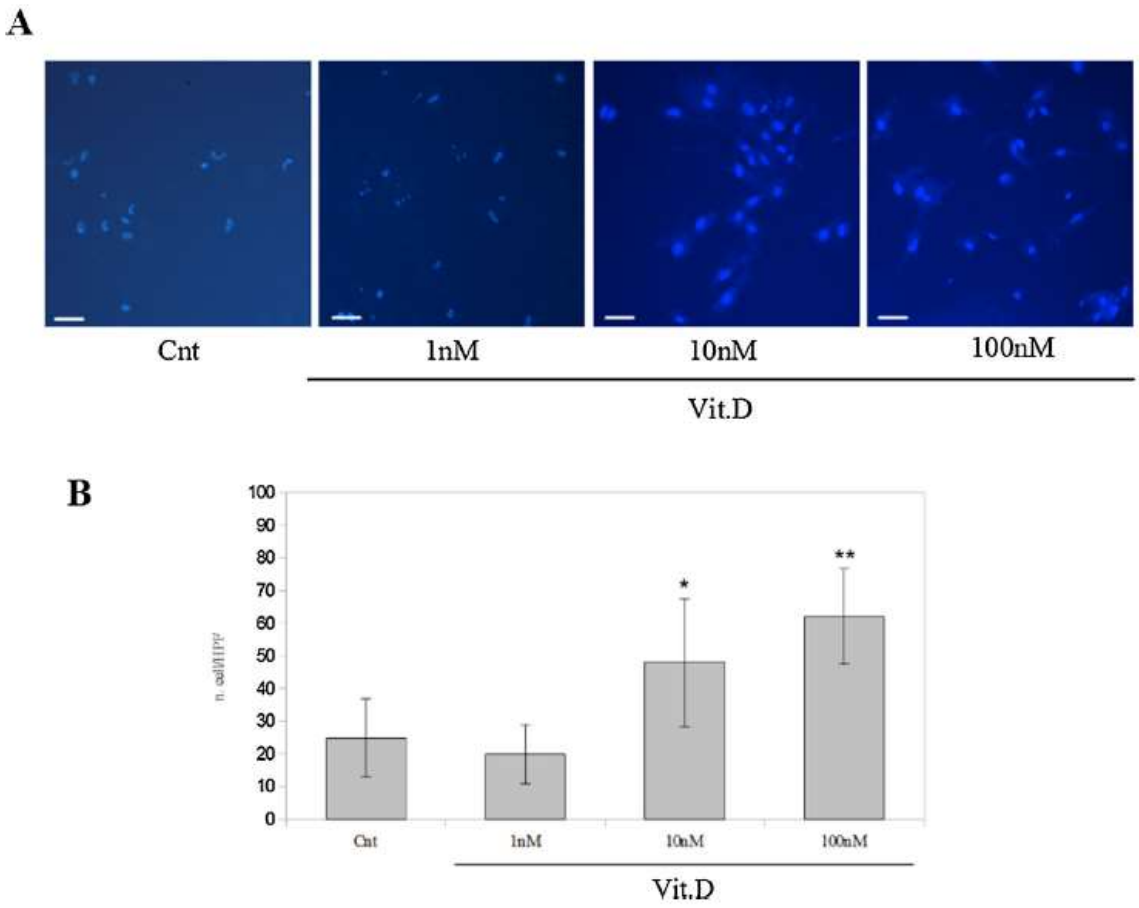

*Figure 11. Vitamin D-treated HUVEC migration into the 3D matrix. A) Fluorescence microscopy images of control and vitamin D (1-10-100 nM) treated cells migrated in the 3D matrix after 7 days of incubation, stained with Hoechst 33342. Original magnification = 10X. Scale bar = 60 μm. B) Determination of HUVEC migration after 7 days of incubation in the presence of different concentration of vitamin D (1-10-100 nM). Results are expressed as n. cell/HPF ± S.D. One-way ANOVA followed by Bonferroni post-test were used for statistical analysis. *p<0.05; **p<0.01.*

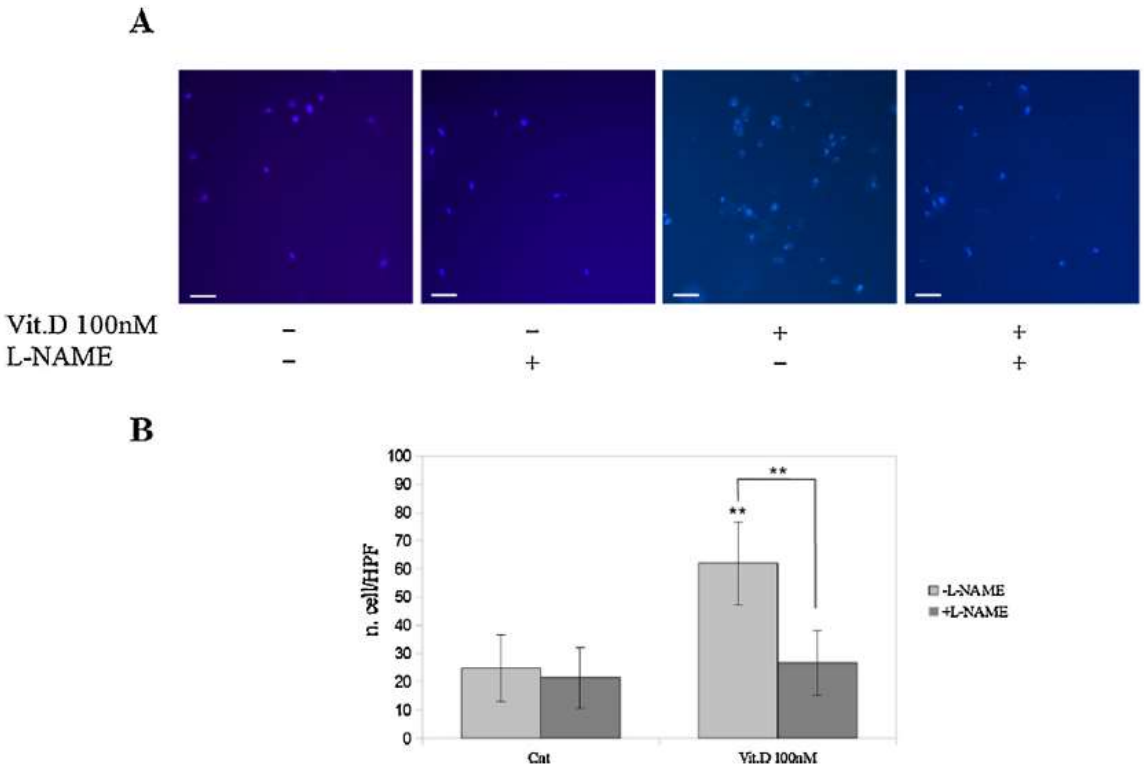

*Figure 12. Vitamin D and L-NAME -treated HUVECs migration into the 3D matrix. A) Fluorescence microscopy images of control and vitamin D (100 nM) treated cells, both in the absence and presence of L-NAME, migrated in the 3D matrix after 7 days of incubation and stained with Hoechst 33342. Original magnification = 10X. Scale bar = 60 μm. B) Determination of control and vitamin D (100 nM) treated cells after 7 days migration both in the absence and presence of L-NAME. Results are expressed as n. cell/HPF ± S.D. One-way ANOVA followed by Bonferroni post-test were used for statistical analysis. **p<0.01.*

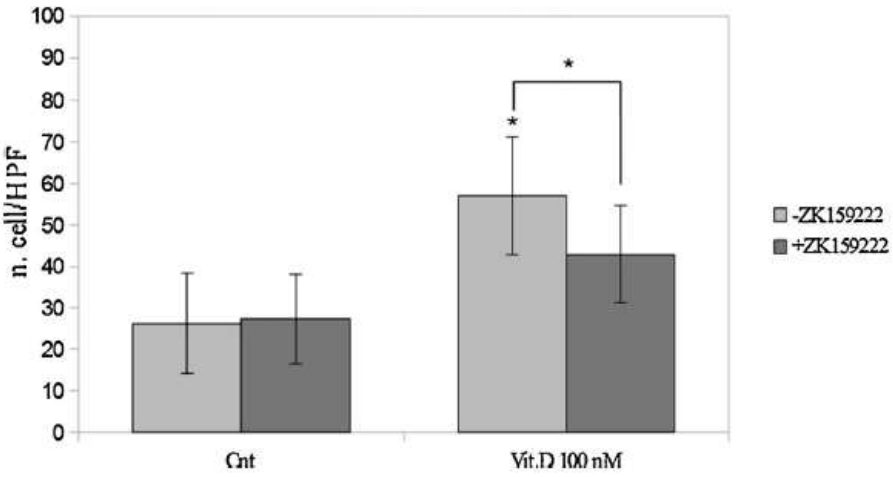

*Figure 13. Vitamin D and ZK159222-treated HUVECs migration into the 3D matrix. Determination of control and vitamin D (100 nM)-treated cells after 7 days migration both in the absence and presence of ZK159222. Results are expressed as n. cell/HPF ± S.D. One-way ANOVA followed by Bonferroni post-test were used for statistical analysis. *p<0.05.*

Vitamin D induces MMP-2 expression via NO-dependent pathway

Extracellular matrix degradation is one of the main steps in cell migration; for this reason vitamin D effects on MMP-2 expression in the conditioned medium of cells migrating into the 3D hydrogel matrix after 7 days has been evaluated by gelatin zimography.

As shown in Figures 14A and 14B, vitamin D addition to PAE cultures medium increases MMP-2 production in a dose-dependent manner. In HUVECs, gelatin zymography demonstrates a statistically significant increase in MMP-2 activity in all the vitamin D-treated samples (Figure 15). This effect is more evident in samples stimulated with 100 nM vitamin D ($p<0.01$). The increase in MMP-2 expression appears to be NO dependent, as L-NAME treatment totally abrogates vitamin D effects on MMP-2 expression (Figures 14C and 14D for PAE cells; Figure 15 for HUVECs), according to the results described above for cell migration.

In ZK159222-treated samples, MMP-2 activity in HUVECs reflects the data obtained for the migration assay (Figure 16).

Furthermore, Vitamin D effects on MMP-2 mRNA expression after 24 h of stimulation with the most effective vitamin D concentration (100 nM) was investigated in HUVEC cultures. As shown in Figure 17, vitamin D is able to induce a statistically significant increase in MMP-2 mRNA expression. As expected, L-NAME treatment decreases vitamin D-induced effects on MMP-2 mRNA expression (Figure 17).

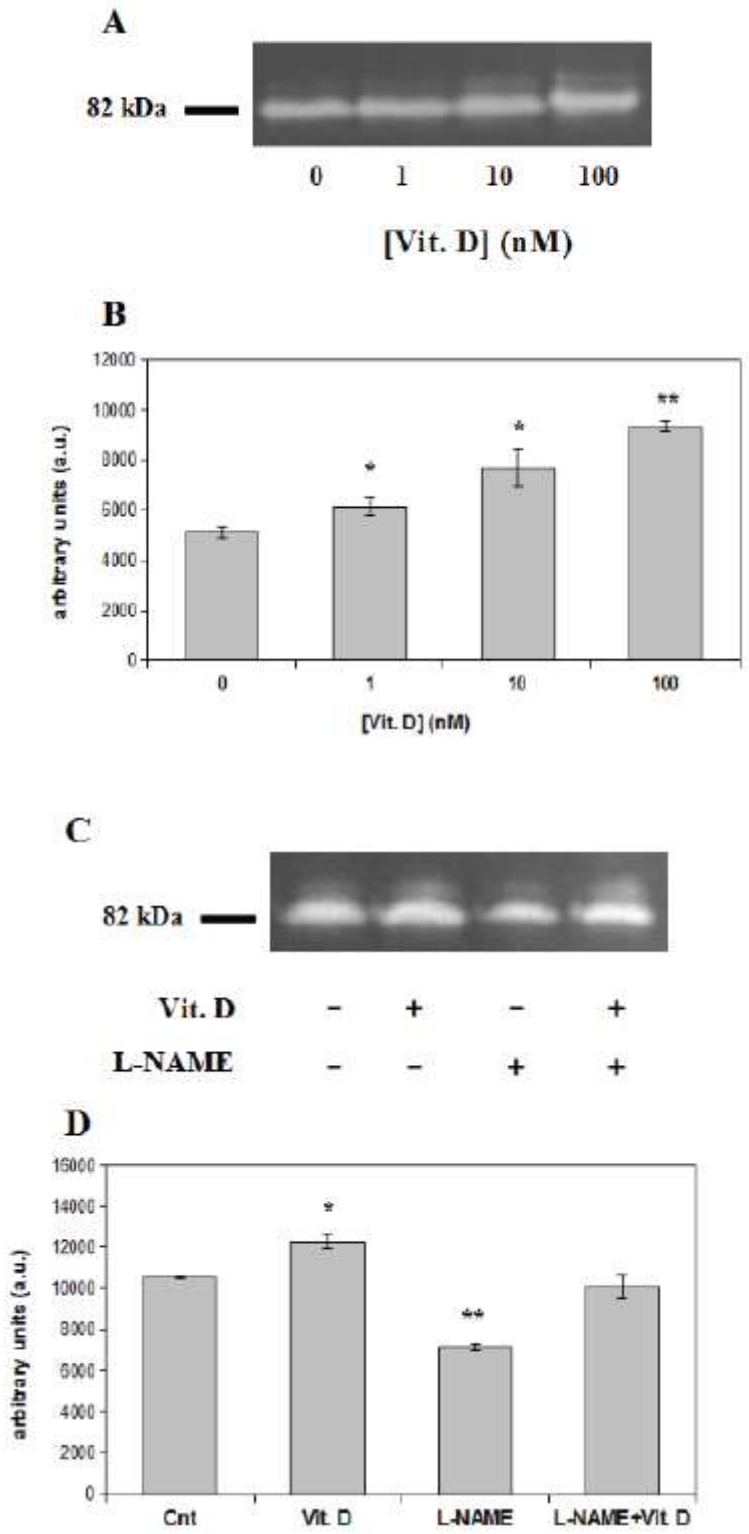

Figure 14. MMP-2 production in PAE cells. A) Representative zymography of cell growth medium from PAE cells migrated into the 3D matrix for 7 days in the presence of different vitamin D concentrations (1-10-100 nM). B) Densitometric quantification of MMP-2 expression. C) Representative zymography of cell growth medium from control and vitamin D

(100 nM) PAE cells migrated into the 3D matrix for 7 days, both in the presence or absence of L-NAME. D) Densitometric quantification of MMP-2 expression.

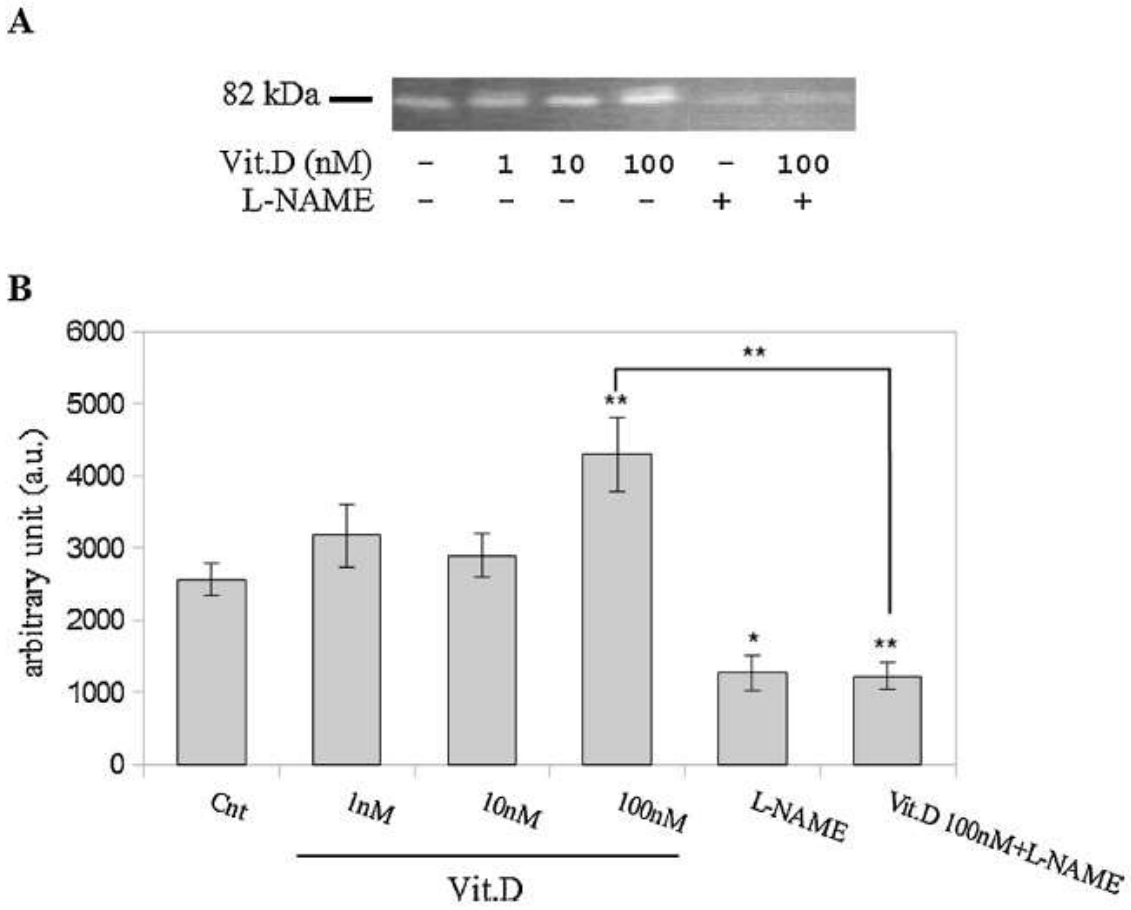

*Figure 15. MMP-2 activity in vitamin D and L-NAME-treated HUVECs. A) Representative zymography of cell growth medium from vitamin D-treated HUVEsC migrated into the 3D matrix for 7 days in the absence or presence of L-NAME. B) Densitometric quantification of MMP-2 expression. One-way ANOVA followed by Bonferroni post-test were used for statistical analysis. *p<0.05; **p<0.01.*

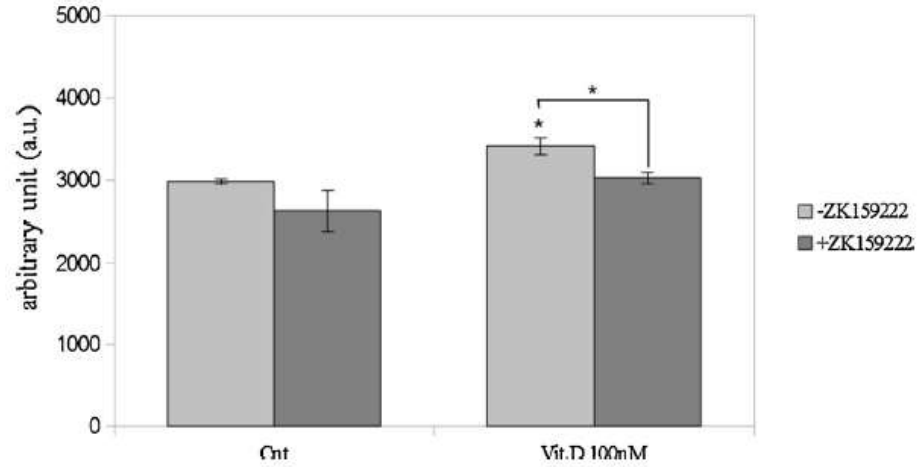

*Figure 16. MMP-2 activity in vitamin D and ZK159222-treated HUVECs. Densitometric quantification of MMP-2 expression. One-way ANOVA followed by Bonferroni post-test were used for statistical analysis. *p<0.05.*

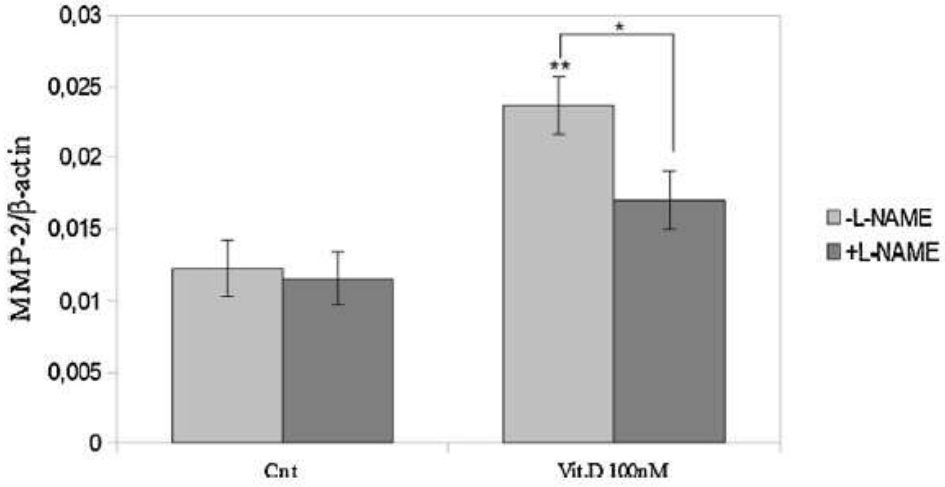

*Figure 17. MMP-2 mRNA expression in HUVECs. Densitometric quantification of MMP-2 mRNA expression of control and vitamin D (100 nM)-treated cells in the absence or presence of L-NAME after 24 h of incubation. Results are expressed as MMP-2/β-actin ratio ± S.D. One-way ANOVA followed by Bonferroni post-test were used for statistical analysis. *p<0.05; **p<0.01.*

Vitamin D effects on cell viability during oxidative stress condition

In the same experimental conditions used for NO production, cell viability was evaluated through MTT test in HUVEC cultures.

After stimulation with 1 nM of vitamin D alone, cell viability shows a significant increase of approximately 18.57 ± 2.13 % ($p<0.05$), and in combination with 1 nM ZK191784 this effect is amplified of about 39.5 % (25.91 ± 1.02 %, $p<0.05$; Figure 18). These data indicate vitamin D ability to increase cell viability in physiological conditions. Pretreatment with H_2O_2 for 20 min causes a reduction in cell viability (9.77 ± 0.91 %, $p<0.05$), that was prevented only by pretreatment with 1 nM of vitamin D alone (13.16 ± 1.37 % compared with controls) or in combination with 1 nM ZK191784 (16.95 ± 1.66% compared with controls; Figure 18). This effect is similar to what is observed for NO production.

For this reason, we hypothesize that vitamin D is able to prevent the negative effects of H_2O_2 only if it is used before the oxidative stress.

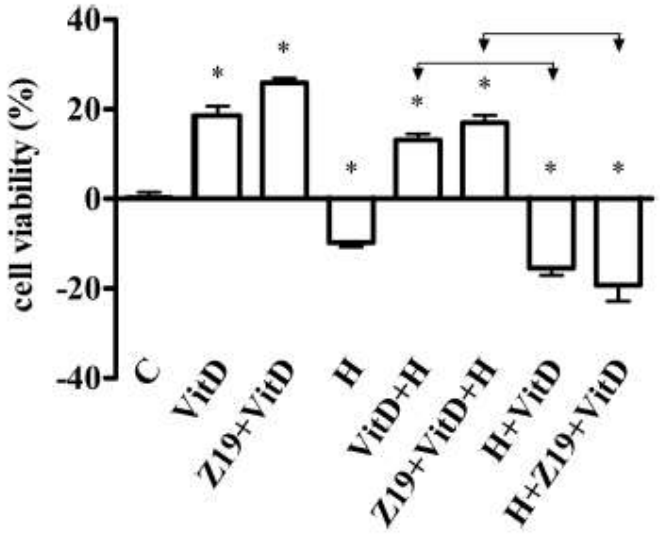

*Figure 18. Effects on cell viability determined by means of MTT test, induced by vitamin D (VitD; 1nM) alone or in combination with ZK191784 (Z19; 1 nM) and/or H_2O_2 (H; 200 μM) in HUVEC cultures. C=control; Z19+VitD, VitD+H, Z19+VitD+H, H+VitD, H+Z19+VitD=combination. * p<0.05 vs control; arrows indicate H+VitD p<0.05 vs VitD+H and H+Z19+VitD p<0.05 vs Z19+VitD+H. Data are means (%) ± S.D. of 5 independent experiments.*

Vitamin D effects on ROS production during oxidative stress condition

In HUVECs treated with 1 nM of vitamin D alone or in combination with 1 nM ZK191784, significant changes in superoxide anion production compared with controls are not observed; in the sample treated with hydrogen peroxide the superoxide anion production is increased to 23.08 ± 1.17 nmol per reduced cytochrome C per μg of protein ($p<0.05$) from control values of 4.7 ± 1.096 nmol per reduced cytochrome C per μg of protein (Figure 19). Pretreatment with 1 nM of vitamin D alone reduces superoxide anion production ($p<0.05$), and this effect is amplified of 19.7% ($p<0.05$) in the presence of 1nM ZK191784 (15.17 ± 0.38 and 12.19 ± 1.6 nmol per reduced cytochrome C per μg of protein, respectively; Figure 19). Stimulation with vitamin D alone or in combination with ZK191784 after treatment with hydrogen peroxide do not induce an important superoxide anion reduction compared to the effect of H_2O_2 alone ($p<0$ .05; Figure 19).

These data confirmed previous findings on NO production and the MTT test, and demonstrate the ability of vitamin D to prevent the negative effects of oxidative stress only if it used before the oxidative event.

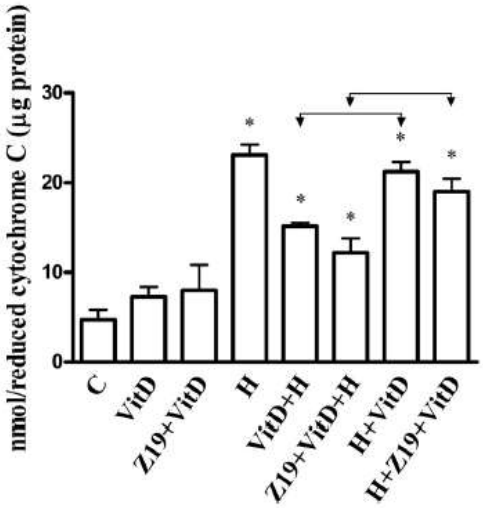

*Figure 19. Effects on reactive oxygen species production induced by vitamin D (VitD; 1nM) alone or in combination with ZK191784 (Z19; 1 nM) and/or H_2O_2 (H; 200 μM) in HUVEC cultures undergoing oxidative stress condition. The abbreviations are the same used in previous figures. * $p<0.05$ vs control; arrows indicate H+VitD $p<0.05$ vs VitD+H and*

H+Z19+VitD p<0.05 vs Z19+VitD+H. Data are means (%) ± S.D. of 5 independent experiments.

Vitamin D counteracts apoptosis caused by hydrogen peroxide through activation of autophagic and survival signaling

The same experimental protocol previously described was used to treat HUVECs in order to investigate the mechanisms activated by vitamin D during the oxidative stress.

The stimulation with vitamin D alone induces significant changes ($p<0.05$) in apoptosis- and autophagy-associated proteins expression.

It reduces apoptotic marker expressions such as Bax, caspase-3, caspase-8, caspase-9, and cytochrome C compared with control samples, investigated using Western Blot analysis ($p<0.05$; Figures 20 and 21). These data are confirmed by immunofluorescence for caspase-3, immunocytochemistry for annexin V and TUNEL assay (Figure 22), confirming a protective role of vitamin D from cell death.

In addition, vitamin D increases Beclin 1, ERK 1/2 and Akt expressions compared with control samples ($p<0.05$; Figures 20 and 21), investigated using Western Blot analysis. Beclin 1 is involved in the autophagic pathway, while ERK 1/2 and Akt in the RISK (Reperfusion Injury Salvage Kinase) pathway.

Graded and amplified changes in apoptosis and autophagy expression are found also in the presence of vitamin D plus the VDR agonist ZK191784; a reduction of Bax, caspase-3, caspase-8, caspase-9, annexin V, TUNEL, and cytochrome C expressions and an increase of Beclin 1, ERK 1/2, and Akt expressions are observed ($p<0.05$; Figures 20, 21, and 22).

Samples treated with H_2O_2 alone shows the opposite characteristics; the expressions of all the markers of apoptosis tested are increased compared with controls ($p<0.05$), and the signaling of survival markers is decreased (Figures 20, 21 and 22).

Similar data are obtained in a caspase-3 activity test (Figure 21F), in which vitamin D alone caused a reduction of caspase-3 activity (-4.48 ± 0.78 %; $p<0$ .05); in combination with ZK191784, this effect is amplified (-5.67 ± 2.08 %; $p<0.05$). The stimulation with H_2O_2 alone induces a significant increase in caspase-3 activity to control values (41.46 ± 1.46%; $p<0.05$). The pretreatment with vitamin D alone or in combination with ZK191784 is able to prevent the activity of caspase-3 during oxidative stress (3.5 ± 1.5 % and 2.6 ± 0.6 %, respectively), but the same stimulation after treatment with H_2O_2 does not reverse the effect (50.26 ± 1.78 %

and 50.67 ± 4.16 %, respectively). These results are also confirmed by immunofluorescence analysis (Figure 22).

As shown in Figure 21, pretreatment with hydrogen peroxide and the subsequent vitamin D stimulation alone or co-administered with ZK191784 shows that vitamin D and its agonist reduce the activation of apoptosis and increase the expressions of autophagic and survival signaling compared with H_2O_2 treatment alone.

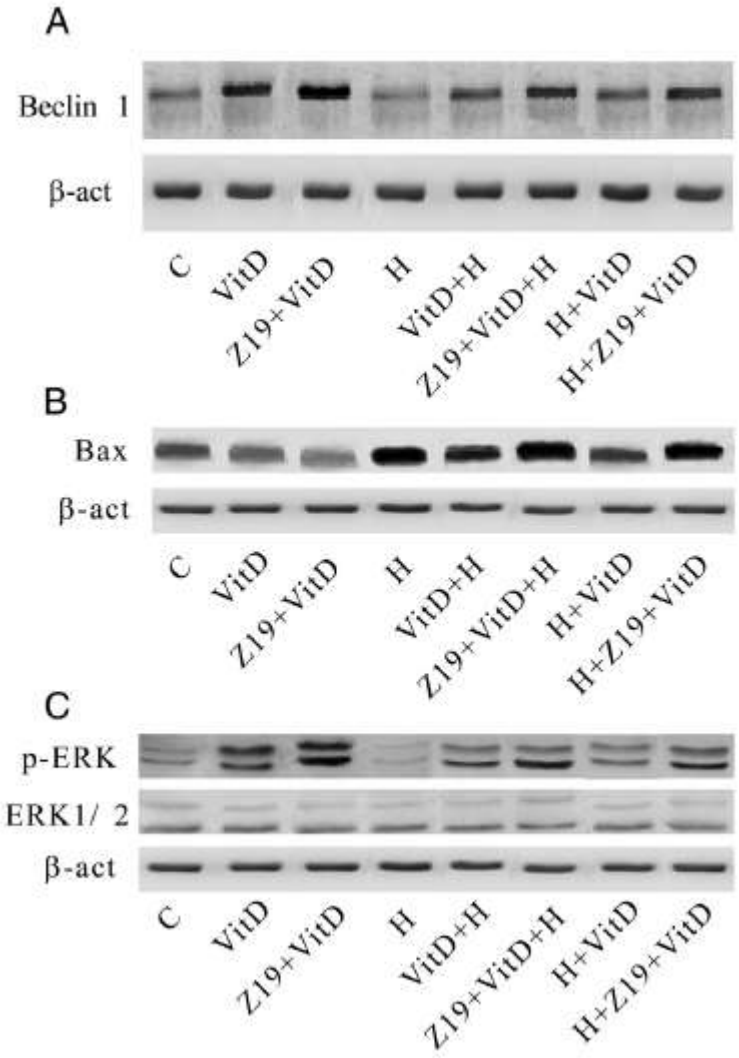

Figure 20. Effects of vitamin D (VitD; 1nM) alone or in combination with ZK191784 (Z19; 1nM) and/or H_2O_2 (H; 200M) on Beclin 1 (panel A) and Bax (panel B) expressions, and ERK1/2 phosphorylation (p; panel C). Immunoblots of activation and phosphorylation relative to the specific proteins are shown. The results represent an example of 5 independent experiments. Abbreviations: β-act=actin.

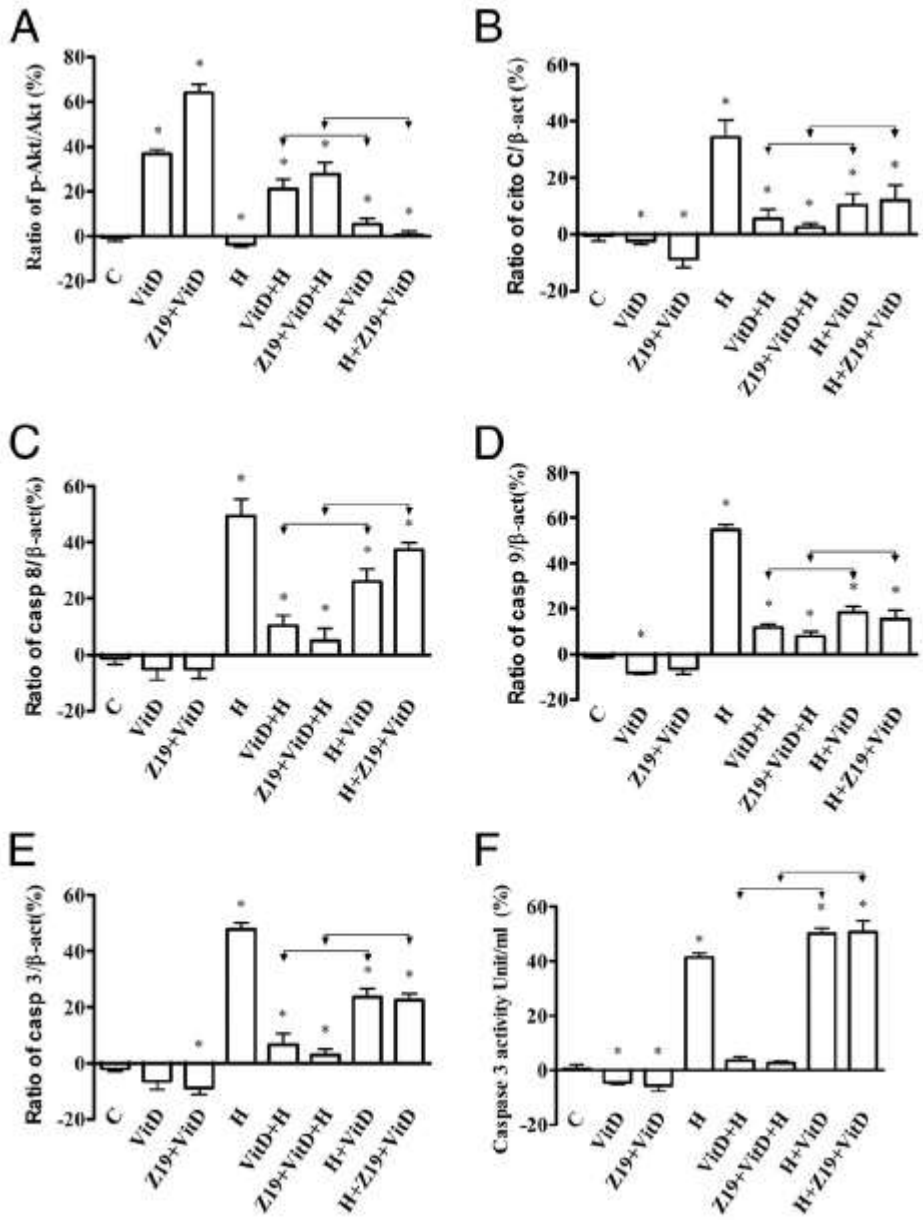

*Figure 21. Densitometric analysis of the effects of vitamin D (VitD; 1nM) alone or in combination with ZK191784 (Z19; 1nM) and/or H_2O_2 (H; 200M) on various kinases. A) Akt phosphorylation. B) Cytochrome C activation. C) Caspase-8 activation. D) Caspase-9 activation. E) and F) Caspase-3 activation and relative protein activity, respectively. * $p<0.05$ vs control; arrows indicate H+VitD $p<0.05$ vs VitD+H and H+Z19+VitD $p<0.05$ vs Z19+VitD+H. Data are means (%) ± S.D. of 5 independent experiments.*

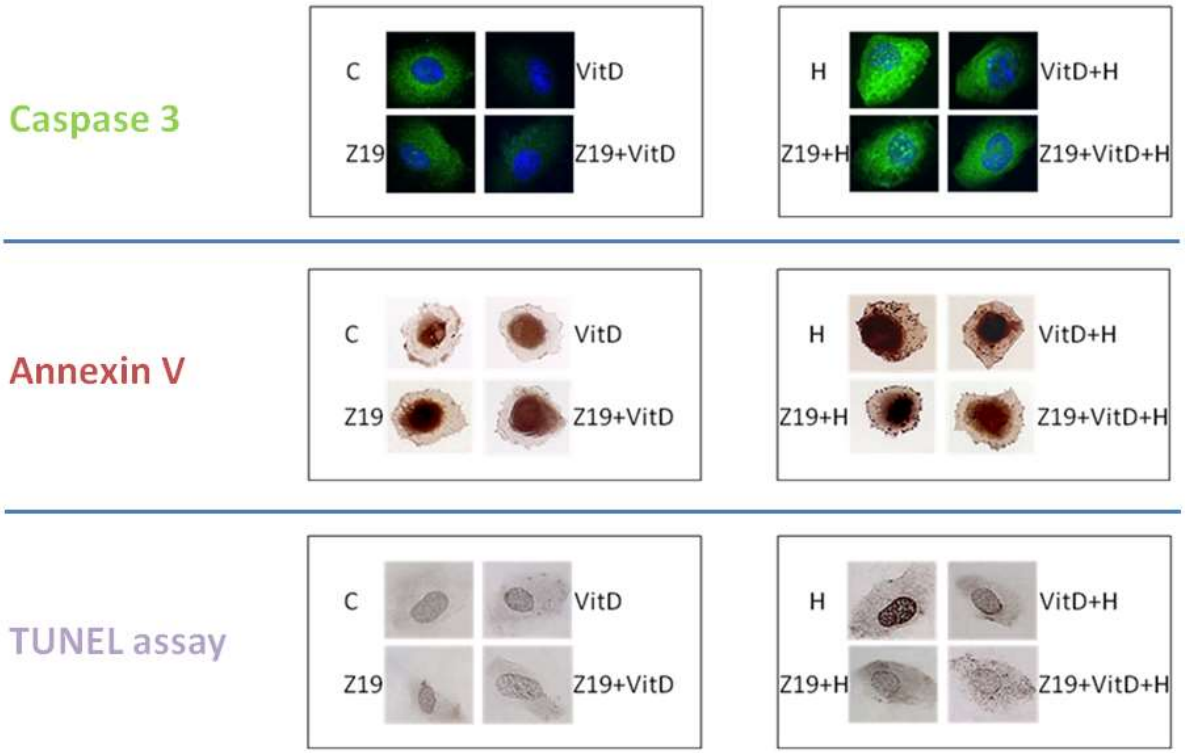

Figure 22. Vitamin D effects on apoptotic marker expression. The top of the panel shows Caspase-3 immunofluorescence (in green; nuclei are counterstained in blue with DAPI). In the middle of the panel, Annexin V immunocytochemistry. At the bottom of the panel, TUNEL assay. Abbreviations are the same as used before. Example of 5 independent experiments; original magnification 40 X.

Vitamin D effects on mitochondrial membrane potential (MMP) and mitochondrial permeability transition pore (MPTP) opening during oxidative stress

As shown in Figure 23A, 1 nM vitamin D is able to prevent (45.33 ± 8.39 %, $p<0.05$) the loss of mitochondrial membrane potential induced by H_2O_2 (-11 ± 4.58 %), and this effect is amplified in the presence of ZK191784 (71 ± 3.61 %, $p<0.05$).

These results demonstrate that vitamin D could prevent the loss of mitochondrial membrane potential through the modulation of apoptosis/autophagy pathways.

Moreover, additional experiments were performed to examine the modulation of MPTP opening. As reported in Figure 23B, stimulation with H_2O_2 causes a significant reduction ($p<0.05$) of mitochondria-trapped calcein intensity (-34 ± 5.92%; $p<0.05$), which is prevented by treatment with vitamin D, and this effect is amplified in the presence of ZK191784 ($p<0.05$). In the samples pretreated with 1 M cyclosporin A, an agent that interacts with cyclophilin D to delay MPTP opening, a significant increase in calcein intensity is observed in the sample stimulated with H_2O_2 alone (28 ± 6.03 %; $p<0.05$); when vitamin D alone or in combination with ZK191784 are added, these effects are amplified (34.03 ± 4 % and 92.33 ± 5.86 % compared with controls, respectively).

In conclusion, the results demonstrate that vitamin D is able to prevent MPTP opening during oxidative stress.

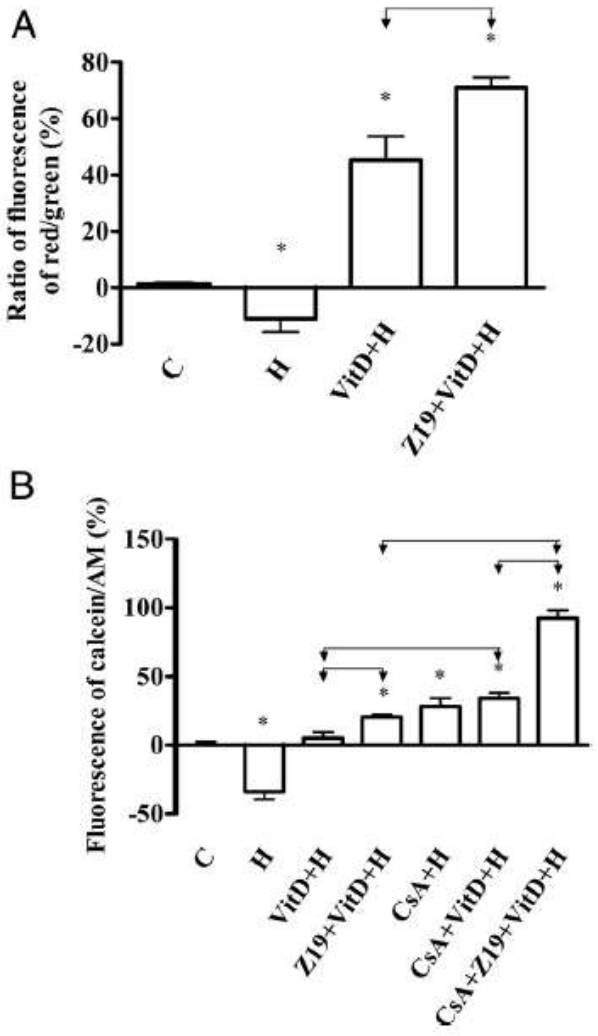

*Figure 23. Study of MMP (panel A) and MPTP opening (panel B) in HUVECs treated with vitamin D (VitD; 1nM) alone or in combination with ZK191784 (Z19; 1nM) and/or H_2O_2 (H; 200M). The abbreviations are the same as used in the previous figures. Csa=cyclosporin A. Calcein/AM=acetomethoxy derivate of calcein. In panel A: * p<0.05 vs control; arrows indicate Z19+VitD+H p<0.05 vs VitD+H. In panel B: *p<0.05 vs control; arrows indicate Z19+VitD+H p<0.05 vs VitD+H. CsA+VitD+H p<0.05 vs V+H; CsA+Z19+VitD+H p<0.05 vs Z19+VitD+H; CsA+Z19+VitD+H p<0.05 vs CsA+VitD+H. Data are expressed as means (percentage) ± S.D. of 5 independent experiments.*

DISCUSSION

Steroid hormones exert several effects in many organs and tissues; thus, many different actions, beyond vitamin D predominant and well-known functions on bone and mineral homeostasis, have been demonstrated. Indeed, the diffused presence of VDR and vitamin D-metabolizing enzymes in about all cells and tissues, and the very large number of genes that are directly and/or indirectly responsive to $1,25(OH)_2D_3$-VDR complex point toward this role. In particular, the association between vitamin D deficiency and cardiovascular diseases has been deeply investigated in clinical trials (80, 81) and recently vitamin D has been proposed as a novel and effective approach for vascular regeneration (82). Moreover, angiogenesis, a multistep process including ECs proliferation and migration into surrounding stroma/tissues, is dysregulated in different pathologies, such as cardiovascular diseases, diabetes and chronic inflammation (83, 84).

For this reason our aim was to investigate the cardiovascular system, in particular the endothelial cells, in physiological condition and during oxidative stress, in order to clarify vitamin D induced-molecular pathways activated in these processes. In the experimental procedures we used *in vitro* models of PAE cells and HUVECs; especially the latter provide a very good human model for investigations such as angiogenesis, signal transduction and ischemia/reperfusion injury, in comparison with other cell types (85).

In the first part of this study the effects of vitamin D administration in physiological condition in PAE cells and HUVECs have been investigated. A first set of experiments reveal a vitamin D-induced cell proliferation. These effects are actually mediated by VDR and its involvement is confirmed by the absence of increased cell proliferation in the presence of the VDR antagonist ZK159222. In a second set of experiments focused on identifying vitamin D effects on cell migration, a dose-dependent increase in cell migration in the three-dimensional matrix is found.

Angiogenesis requires the presence of proteases, such as endogenous zinc dependent MMPs, which can degrade some of the components of the ECM to let ECs migrate into the surrounding environment (86, 87). Moreover, MMPs also contribute to angiogenesis by detaching pericytes from vessels undergoing angiogenesis, by releasing ECM-bound angiogenic growth factors and by stimulating ECs proliferation (88, 89). In particular, MMP-2 and MMP-9, also known as gelatinases, degrade the main components of the vascular basal lamina (collagen IV, laminin and fibronectin; 90). MMP-2 has received growing attention as

it is the main MMPs involved in angiogenesis (91). Considering the key role of MMP-2 in ECs migration, gelatin zymography analysis was used to investigate this aspect. MMP-2 involvement in PAE cells migration well correlates with previous studies reporting a constitutive MMP-2 expression in endothelium (86, 90) and upregulation during ECs migration and tube formation in a 3D matrix (91). Furthermore, after 7 days of cell migration in the 3D matrix, MMP-2 activity in HUVECs is significantly increased in vitamin D-treated samples. L-NAME treatment does not affect control MMP-2 expression, whereas significantly reduces vitamin D-induced effects in both PAE cells and HUVECs. To demonstrate VDR involvement in these effects, some samples were co-stimulated with vitamin D and ZK159222 in HUVECs. This VDR ligand reduces the vitamin D-induced migratory effect. MMP-2 expression was also evaluated by RT-PCR in HUVECs to determine MMP-2 mRNA expression; the stimulation with the most effective vitamin D concentration for 24 h causes an increase in MMP-2 mRNA expression.

Endothelium-derived NO is a bioregulatory molecule that controls the vascular tone and it is a critical mediator of angiogenic process (92, 93). Vitamin D effects on cell proliferation are related to NO balance, as it regulates many different processes, such as ECs survival, proliferation and migration, and the expressions of VEGF and FGF from vascular cells leading to an increase in angiogenic stimuli (83, 94). Co-presence of vitamin D and its synthetic antagonist ZK159222 result in an almost complete inhibition of vitamin D-mediated NO production. The correlation between vitamin D stimulation and NO production in PAE cells is confirmed by eNOS inhibition, induced using the competitive inhibitor L-NAME, resulting in an effective vitamin D antagonistic effect activity on cell proliferation and migration. As expected, L-NAME prevents vitamin D-induced cell proliferation and migration also in HUVECs, drastically reducing cell number. Moreover, L-NAME causes a dramatic reduction in MMP-2 activity confirming the involvement of NO as a mediator of vitamin D effects.

A schematic view of the results of this first part of the study is summarized in Figure 24.

Furthermore, in the second part of this research, the mechanism activated by vitamin D to counteract the negative effects induced by oxidative stress in ECs was investigated. As reported in the literature, vitamin D reduces the damage induced after H_2O_2-mediated stress in a dose- and time-dependent manner through the decrease of anion superoxide generation and apoptotic cells formation (95). In the present study, it has been clearly demonstrated that vitamin D administration to ECs before induction of an oxidative stress could improve cell

viability. The mechanisms involved include the prevention of free oxygen radical release and the modulation of the interplay between apoptosis and autophagy. These effects are accompanied by NO production and preservation of mitochondrial function. In these experiments, HUVEC cultures received an oxidative stress by means of H_2O_2. This method is widely used to reproduce a cellular damage similar to what occurs in myocardial ischemia/reperfusion injury (65). In light of these data, a cardioprotective role of vitamin D against the ischemic injury can be hypothesized. As observed in NO production and MTT tests, the effect induced by VDR agonist ZK191784 is greater than the one observed after vitamin D stimulation alone. Moreover, the combined administration of vitamin D and ZK191784 causes an amplified effect and going deeply in this item could be an interesting issue for future researches. These beneficial effects are observed when the VDR agonists were administered before the induction of oxidative stress. This finding supports the hypothesis that vitamin D is able to counteract the negative effects of the oxidant event on endothelial cells, increasing cell viability.

In addition, vitamin D-induced NO release during oxidative stress protects cells from death, since the rate of NO production observed is below 2 μM/s. This threshold prevents the opening of the mitochondrial transition pore and the release of cytochrome C and avoids mitochondrial collapse leading to cell death (96). Oxidative stress plays an important role in the pathogenesis of atherosclerosis (97, 98). In recent years, several studies have indicated that antioxidant vitamins such as vitamin C or E may restore endothelial function and may have anti-inflammatory and antithrombotic properties (99). Moreover, overwhelming evidence demonstrate that NO plays a fundamental biological role in protecting the heart against ischemia/reperfusion injury. Recent investigations on cardiac myocytes show that ROS produced by mitochondrial and oxidative stress could cause multiple changes in cell structure and function, that are associated with heart failing (100), apoptosis (101) or autophagy (102). The antiapoptotic effects of NO and ROS involvement in several signaling pathways, and the interplay between autophagic and apoptotic pathways is a crucial point to determining the initiation of programmed cell death. Pretreatment with vitamin D, alone or in combination with ZK191784, reduces apoptosis-related gene expression (Bax, caspase-3, caspase-9, caspase-8, and cytochrome C), involving both the intrinsic and the extrinsic pathways. These findings are confirmed by immunohistochemistry analysis of annexin V and TUNEL assay, in which a reduction of the signal is observed. At the same time, activation of pro-autophagic Beclin 1 and phosphorylation of ERK1/2 and Akt, members of the reperfusion

injury salvage kinase pathway, has been demonstrated, indicating a modulation between apoptosis and autophagy. Moreover, vitamin D administration alone or in combination with ZK191784 used before the oxidative stress event prevents the loss of mitochondrial potential and the consequent cytochrome C release and caspase activation. Vitamin D alone or in combination with ZK191784 is able to prevent the MPTP opening caused by H_2O_2. These findings depend on changes of mitochondria-trapped calcein intensity and effects of cyclosporin A, which inhibits MPTP opening, modulating the cyclophilin D activity (99).
A schematic view of the results of this second part of the study is summarized in Figure 25.

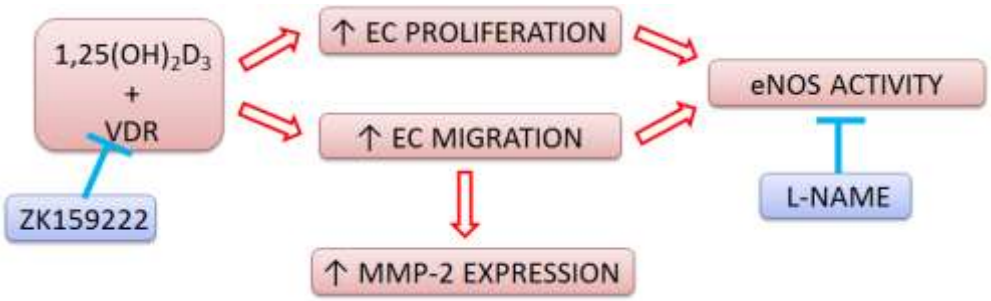

Figure 24. Schematic view of the results regarding vitamin D effects on ECs proliferation and migration.

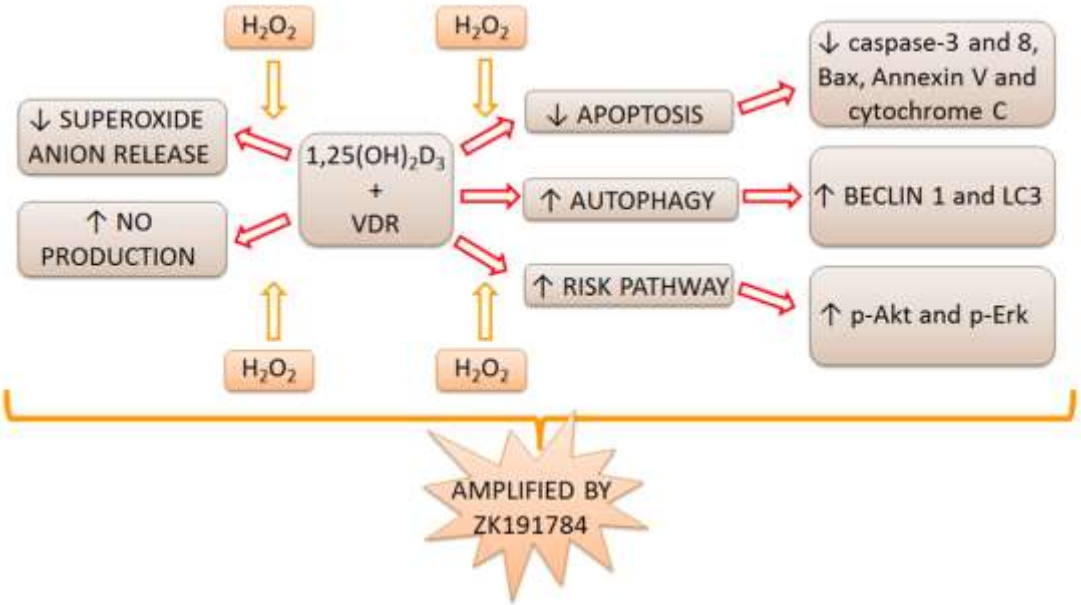

Figure 25. Schematic view of the results regarding the ability of vitamin D to counteract the negative effects induced on ECs by the oxidative stress condition.

CONCLUSION

The results described herein highlight that vitamin D stimulates PAE cells and HUVECs proliferation and migration in a 3D matrix and that these phenomena depend on NO production. Furthermore, this work adds new information to the debate on the benefits of vitamin D supplementation. Indeed it shows for the first time that vitamin D may prevent ECs death through the modulation of the interplay between apoptosis and autophagy. This effect is obtained by inhibiting superoxide anion generation, maintaining mitochondria function and cell viability, activating survival kinases, and inducing NO production.

In the recent years the knowledge about vitamin D have improved and its implications have extended beyond its classical role in bone health in either fields of basic research as well as in human trials, showing the relevance of the vitamin D system. Until now the available data are significant and confirm its essential role in several physiological and preventive functions. In future, we will need to further apply and exploit the vitamin D research to better understand the underlying mechanisms and molecular pathways by which it exerts so many different and fundamental effects in the human body. A greater understanding of vitamin D system will shed new light on vitamin D supplementation in very promising fields such as tissue repair, wound healing and prevention of human angiogenic process.

OTHER TOPICS

Beyond the main line of research on vitamin D, during my PhD period I also productively worked on two other topics.

I collaborated with the Physical and Rehabilitation Medicine Unit (Azienda Ospedaliera Universitaria "Maggiore della Carità", Department of Health Sciences, University of Eastern Piedmont "Amedeo Avogadro", Novara) to study serum myostatin and sclerostin levels in chronic spinal cord injured patients.

Moreover, I also worked with the Department of Obstetrics and Gynecology (Fondazione IRCCS Ca' Granda, Ospedale Maggiore Policlinico, Milan) and the Unit of Pathology in Novara (Department of Health Sciences, University of Eastern Piedmont "A. Avogadro") in order to study iron effects on fimbrial cells.

I briefly describe below what arose from these further researches.

1) EVALUATION OF SERUM MYOSTATIN AND SCLEROSTIN LEVELS IN CHRONIC SPINAL CORD INJURED PATIENTS

Introduction

Spinal cord injury (SCI) is a long-standing and pressing public health problem. In SCI the injury force damages or destroys neural tissue causing sudden loss of neurological functions and several documented complications, such as reduction in bone mineralization, deterioration of skeletal microarchitecture (predominantly in long bones of lower limbs), and unloading, which represents the main determinant of osteoporosis, increasing the risk of fractures (103, 104). Sclerostin, a powerful selective inhibitor of Wingless and Int signaling identified as one of the key regulators of mechanical load responses, is produced by osteocytes and induces a reduction in osteoblast activity and proliferation, resulting in the loss of bone mass. Recently, a strong correlation between bone mineral density (BMD) and serum sclerostin in patients with SCI has been established (105, 106). Furthermore, the evidence of a biochemical and bi-univocal cross-talk between the muscle and the bone has become apparent and satellite cells, together with osteocytes, could have a pivotal role - in particular myostatin, inhibiting muscle differentiation and growth (107-109).

The aim of this study is to assess whether sclerostin and myostatin could possibly be used as biomarkers for osteoporosis and for the evolution of muscular modifications in SCI patients, respectively. For this purpose, a case-control study has been designed to estimate serum sclerostin and myostatin concentrations, BMD and appendicular skeletal muscle mass (ASMM) in a population of chronic SCI patients.

Materials and methods

28 patients suffering from chronic SCI were enrolled in the study from the Physical and Rehabilitation Unit in Novara. Inclusion criteria were the following: (1) SCI; (2) a grade from A to C on the American Spinal Injury Association (AIS) Impairment Scale (110); (3) neurological level of lesion from C5 to T12; (4) age > 18; and (5) time from lesion > 24 months. The exclusion criteria were as follow: concomitant diabetes; oral anticoagulation; other concomitant chronic neurological pathologies (of central and/or peripheral nervous system and/or neuromuscular diseases); use of drugs acting on the bone (bisphosphonates, corticosteroids, lithium, anticonvulsant drugs, parathyroid hormone analogs, estrogens, calcium and vitamin D) and muscle (statins) metabolism. Moreover, 15 healthy controls were enrolled with the following inclusion criteria: absence of SCI and/or any other neurological pathologies; absence of musculoskeletal pathologies; absence of functional limitations (such as gait limitation); age > 18; control subjects should not have any intense physical activity at least in the 24 h before serum sample collection. The exclusion criteria were the same as those of patients suffering from SCI. All study participants signed informed consent forms and the Institutional Review Board approved the study, which was conducted in accordance with the Declaration of Helsinki guidelines.

At baseline all patients underwent a physical examination by a trained physician, and sensory-motor impairment was determined using the AIS impairment scale (111, 112). According to the obtained score, patients were divided in two groups: complete motor (AIS A, B) and incomplete motor (AIS C) subjects. For patients with SCI, the level of disability was measured with the SCIM-III scale (113). After enrollment, all patients underwent blood sample and BMD measurement in the same morning.

Blood samples were collected at the same hour in the morning in fasting conditions. Samples were centrifuged for 15 min at 3000 r.p.m. at 4°C and stored at -80°C until final analysis. Serum plasma iodized calcium, phosphate, creatinine, PTH, 25(OH)D_3, IGF 1, C reactive protein, osteocalcin and Beta-Crosslaps were measured. Myostatin was quantified by the Elisa assay (MyBioSource, San Diego, CA, USA, MBS703668; normal range: 0.625–20 ng/ ml; minimum detectable dose 0.312 ng/ml). Serum sclerostin was measured using the SOST Elisa Kit (Biomedica Gruppe, Vienna, Austria; normal range: 0–240 pmol/l; detection limit: 2.6 pmol/l; unit conversion of 1 pg ml/l=0.044 pmol/l). Whole-body tetrapolar bioelectrical impedance analysis (BIA) was performed using an alternating sinusoidal electric current of 400 mA at a single operating frequency of 50 kHz (BIA 101 Anniversary Sport Edition-ASE-Akern Srl; Florence, Italy). The device's precision was 1 % for resistance and 5 % for reactance. BIA was performed with supine subjects with their limbs slightly away from their body, after an overnight fast, and bladder voiding. To avoid inter-observer errors, all BIA measurements were taken by the same investigator (MI). Active electrodes (BIATRODES Akern Srl; Florence, Italy) were placed on the right side on conventional metacarpal and metatarsal lines, recording electrodes in standard positions at the right wrist and ankle. All resistance measurements were normalized for stature (height in centimeters squared/resistance) to obtain the resistive index (RI). ASMM was obtained using a validated equation (114). Then, the ASMM index (ASMMI) value was obtained using the following calculation: ASMM/height. BMD of patients and healthy controls was measured with calcaneus ultrasonography (Achilles Express 2001 GE Medical System, Lunar Corporation-Madison, WI, USA), obtaining data about T-score and stiffness.

Statistical analyses were performed using the GraphPad 4 package, version 4.0 (GraphPad Software, Inc., San Diego, CA, USA). Because of the small sample size, we assumed a non-gaussian distribution of the considered variables. After enrollment, patients were divided into two subgroups, depending on motor completeness of the lesion (complete and incomplete). Differences between single variables in different groups were evaluated with the Mann-Whitney U-test. A type I error level of 0.05 was chosen. The Bonferroni correction for multiple comparisons was applied considering three variables, which resulted in a new alpha-error level of 0.017. Relationships among serum myostatin values and the other variables were analyzed with linear regression using Pearson’s correlation coefficients. Regression

lines were compared using confidence intervals. A $p<0.017$ was considered statistically significant.

Results

Patients with SCI show statistically significant differences regarding smoke, age and history of previous fractures at any site compared with healthy controls, whereas all the other demographical variables reveal no statistical differences. Serum myostatin levels are statistically higher ($p<0.01$) in patients suffering from SCI compared with healthy controls. Similar results have been obtained comparing both patients with motor complete and motor incomplete SCI to healthy controls. Serum sclerostin is significantly higher in SCI patients compared with healthy controls ($p<0.01$). Regarding other biochemical variables, PTH and C reactive protein serum values show statistically significant differences between the two groups; however, the mean values in both groups are in the normal ranges. $25(OH)D_3$ serum levels are significantly higher in healthy controls compared with patients with SCI; however, the mean value in the control group is far from the normal range and only 20 % of healthy controls reveal values of calcidiol higher than 30 ng/ml. Conversely, $25(OH)D_3$ values are <10 ng/ml in 50 % of SCI patients. BMD, stiffness and mean T-score values in SCI patients are significantly lower than those in healthy controls.

Interestingly, we also observe a statistically significant difference between the motor complete and incomplete subgroups regarding these variables. Serum myostatin concentrations in the motor complete SCI subgroup (n=22) correlate only with serum sclerostin levels ($r^2=0.42$; $p=0.001$). None of the other instrumental, biochemical or demographical variables considered show any correlation with serum myostatin concentrations.

Moreover, 10 patients with motor complete SCI (AIS A and B) and 7 healthy controls performed whole-body BIA evaluation. Mean ASSMI in patients with SCI is lower to those of healthy subjects (7.29 ± 1.97 vs 8.01 ± 0.95 Kg/m^2). This difference is not statically significant, but the sample size of this subgroup is extremely small. We found a strong correlation between serum myostatin concentrations and ASMMI in patients with complete SCI ($r^2 = 0.70$; $p=0.002$) but not in healthy controls.

Discussion and Conclusion

Our data point out a statistically significant difference in serum myostatin concentration in SCI patients compared with healthy controls; thus, SCI patients, considering both motor complete and incomplete subgroups, show higher serum values of myostatin compared with healthy controls. To our knowledge, this is the first study investigating serum myostatin levels in SCI patients. Similarly, we observe a significant increase in serum sclerostin levels in chronic SCI patients compared with healthy subjects, confirming findings described in a previous study (106). Moreover, the differences at the bone tissue level among SCI patients and healthy controls are confirmed also by a huge statistically significant reduction in BMD measured at the calcaneus level between these two groups. Finally, serum myostatin correlates only with serum sclerostin (r^2=0.42) and ASMMI (r^2=0.70) in SCI patients, but not in healthy controls.

Circulating biomarkers have been advocated as a useful surrogate measure for diagnosis, therapeutic monitoring and research purposes, considering that they can be easily and noninvasively obtained and that they have a low economic cost.
In conclusion, our results are encouraging, suggesting myostatin as a potential biomarker of muscular modifications and a possible therapeutic target to prevent pathological modifications, not only in SCI patients, but also in other pathological unloading conditions.

2) FIMBRIAL CELLS EXPOSURE TO CATALYTIC IRON MIMICS CARCINOGENIC CHANGES

Introduction

Ovarian cancer affects more than 200000 women worldwide every year with a high mortality rate (115-117). Recent studies have hypothesized fallopian tubes, in particular the secretory epithelial cells in the distal site of tubes, to be the site where most serous ovarian neoplasms develop (118-121).
In the ‘‘incessant menstruation’’ hypothesis, Vercellini and colleagues (118) suggest that the fimbriae, being chronically wetted by peritoneal fluid and by refluxed blood products contained in the pouch of Douglas, are exposed to the action of free radicals and other

metabolites that could promote carcinogenesis. Blood from ovulation and retrograde menstruation could represent the possible pathogenic pathway leading to the development of different cancer histotypes in fertile women, and may explain why fimbria is a site of most serous malignancies (118, 122-124).

Many experimental studies demonstrate catalytic iron-induced carcinogenesis; moreover ovarian endometriotic cysts are rich in catalytic iron (Fe^{3+}), leading to increased oxidative DNA damage (123, 125).

To evaluate the possible role of catalytic iron in the pathogenesis of ovarian carcinoma, in vitro primary fimbrial secretory epithelial cells (FSECs) were analyzed after exposition to Fe^{3+}.

Materials and methods

Fresh fallopian tube fimbriae were obtained from 33 women who attended the endoscopic surgical service of the II Department of Obstetrics and Gynecology of the Fondazione IRCCS Ca` Granda, Ospedale Maggiore Policlinico (Milan, Italy) to undergo isteroannessiectomy for ovarian cancer and benign pathology without comorbidity. All subjects were in premenopause and had not received any type of hormonal or drug therapy for at least 3 months, and gave informed consents. The local human institutional investigation committee granted the approval for the study.

Experiments were performed using physiological concentrations of catalytic iron on FSECs ranging from low doses (0.05, 0.075, and 0.1 mM) to high doses (50, 75, and 100 mM). FSECs were incubated for 2 hours in DMEM without red phenol supplemented with 1% penicillin/streptomycin, 2 mML-glutamine, and 0.5 % FBS before and during the treatments with Fe^{3+} (iron III nitrate nonahydrate; Sigma, Milan, Italy). In the first set of experiments, the stimulation were maintained for up to 144 h and were stopped and analyzed every 24 h. In the second set of experiments, cells were stimulated uninterruptedly for 144 hours, and then maintained in complete medium for 2 or 4 weeks without iron. MTT test, Griess assays, western blotting, immunocytochemistry, immunohystochemistry and immunofluorescence analysis were performed.

Results

The cells acquire an elongated phenotype with low doses of catalytic iron after 48 h of treatment, and immediately in the presence of high doses of Fe^{3+}. High doses of catalytic iron from 120 to 144 h cause evident damages; in particular, cell alteration, with evident loss of cell border, which is a clear indication of plasma membrane oxidative damage.

Both low and high doses of Fe^{3+} significantly reduce the percentage of proliferating cells from 48 to 72 h. After 96 h, cell viability significantly increase ($p<0.05$) and this effect is amplified during the last 2 days in comparison to control cells. These effects result more evident for high doses ($p<0.05$).

In the presence of all doses of catalytic iron, NO production is statistically increased ($p< 0.05$) compared with control during all the 6 days of treatment, and particularly in the presence of high doses of catalytic iron after 72 h.

In the presence of low doses of catalytic iron, p53, pan-Ras, Ki67 and c-Myc activations are observed in a dose-dependent and time-dependent manner; these effects are more evident in the presence of high doses of catalytic iron ($p<0.05$). The highest p53, pan-Ras, Ki67 and c-Myc expressions are evident at 144 h ($p<0.05$) both for 0.1 mM and 100 mM iron concentrations compared with control values. A dose-dependent and time-dependent ERK1/2 and Akt phosphorylations are observed, and these effects are more evident in the presence of high doses of catalytic iron. Similar data are also observed using immunofluorescence for p53 and immunocytochemistry for pan-Ras, Ki67 and c-Myc. After 6 days, the cells mimic carcinogenic changes, without losing the specific secretory epithelial cells marker PAX8, independently from the iron concentrations used. Furthermore, the presence of the proteins analyzed before was also investigated in healthy fimbrial and serous ovarian carcinomas G3 tissues by immunohistochemistry. Healthy fimbrial tissues show a negative staining for p53, pan-Ras and c-Myc, and express cytoplasmic positivity in the epithelial surface for PAX8, as already state in the literature, and focal positivity for Ki67. Instead, in tumoral tissues a focal positivity in neoplastic cells for p53 and pan-Ras, an intense and diffuse nuclear staining in neoplastic cells for Ki67, and a cytoplasmic positivity for c-Myc are observed.

To verify whether all these effects were stabilized in absence of catalytic iron, cells were maintained in complete medium for 2 weeks after treatment with Fe^{3+}. In the presence of low doses of catalytic iron, cell viability increases; this effect is immediately observed in the samples treated for 24 h and is amplified in a time-dependent manner during all the period of

treatment. In addition, cell viability is inversely proportional to the dose of catalytic iron used. In the presence of high doses of Fe^{3+}, cell viability is statistically increased; these effects are observed after 48 h with 50 mM and 75 mM treatments and after 72 h after with 100 mM treatment. Furthermore, NO production observed in the samples treated with low doses of catalytic iron reveal a minimal variation during all the stimulation period. On the contrary, high doses determine a significant decrease in NO production in a dose-dependent and time-dependent manner.

At the end of the 6 days of treatment, the cultures were maintained for 2 and 4 weeks without catalytic iron to analyze whether protein expression persisted. p53, pan-Ras, Ki67 and c-Myc show a significant increase after both 2 and 4 free weeks ($p<0.05$). In particular, after 2 free weeks the effects are dose-dependent, thus more evident in the presence of high doses of catalytic iron. The highest p53, pan-Ras, Ki67 and c-Myc expressions is shown at 100 mM ($p<0.05$), both for 2 and 4 free weeks. These data are also confirmed by immunofluorescence for p53 and immunocytochemistry for pan-Ras, Ki67 and c-Myc. Finally, PAX8 positivity is confirmed, indicating that primary culture do not phenotypically change over time.

Discussion and Conclusions

The molecular mechanisms involved in the carcinogenic pathway in the secretory epithelial cells of fimbria are still unclear. For this purpose, we develop an experimental model in FSECs to explain the involvement of catalytic iron in carcinogenic changes. In the presence of catalytic iron, FSECs show a dose-dependent and time-dependent increase in cell viability. In addition, we show an oxidative damage in fimbrial cells, as indicated by the increased NO production in culture supernatants. The cells show an elongated phenotype in the presence of catalytic iron, maintaining the specific marker for secretory epithelial cells PAX8. p53, c-Myc, Ras and Ki67 expressions after 6 days with all treatments correlate with an enhanced growth, suggesting a possible epithelial cell transformation. These data are also confirmed by ERK/MAPK and PI3K/Akt analysis, for which an increased phosphorylation rate is observed. After both 2 and 4 free weeks, these activations are not reverted, indicating a stabilization of the signals.

This study suggests an alternative interpretation for the role of menstruation in increasing the risk of epithelial ovarian cancer and could be useful to discover early biomarkers to limit oxidative damages in fimbrial cells.

ABBREVIATIONS

(in alphabetical order)

$1,25(OH)_2D_3$: Dyhydroxyvitamin D3, calcitriol

$1,25D_3$ MARRS: Membrane-associated, rapid-response steroid binding protein

$25(OH)D_3$: 25-hydroxyvitamin D3, calcidiol

AM: Acetomethoxy derivate of calcein

ASMM: Appendicular skeletal muscle mass

ASMMI: ASMM index

ATP: Adenosine triphosphate

BCA: Bicinchoninic acid protein assay

BH_4: Tetrahydrobiopterin

BIA: Bioelectrical impedance analysis

BMD: Bone mineral density

Ca^{2+}: Ion Calcium[2*]

CaBP: Calcium binding protein

cGMP: Cyclic guanosine monophosphate

CO_2: Carbon dioxide

CVD: Cardiovascular disease

CYP: Cytochrome P450

CYP24A1: 24-hydroxylase

CYP27A1, CYP2R1: 25-hydroxylase

CYP27B1: 1α-hydroxylase

DBP: Vitamin D-binding protein

DMEM: Dulbecco's modified eagle medium

DNA: Deoxyribonucleic acid

ECs: Endothelial cells

ECM: Extracellular matrix

EGFR: Epidermal growth factor receptor

EGM-2: Endothelial growth medium-2

eNOS or NOS-3: Endothelial NO-synthase or NO-synthase III

ERK: Extracellular signal-regulated kinases

FAD: Flavin adenine dinucleotide

FBS: Fetal bovine serum

Fe^{3+}: Catalytic iron

FGF-23: Fibroblast growth factor-23

FGFR: Fibroblast growth factor receptor

FMN: Flavin mononucleotide

FSECs: Fimbrial secretory epithelial cells

GMP: Guanosine monophosphate

GPCR: G protein coupled receptors

GTP: Guanosine triphosphate

h: Hour/hours

H_2O_2: Hydrogen peroxide

HIF-1α: Hypoxia-inducible factor-1α

HPF: High power microscope field

HUVECs: Human umbilical vein endothelial cells

IGF1: Insulin-like growth factor

iNOS or NOS-2; Inducible NO-synthase or NO-synthase-2

IU: International unit

L-NAME: Nω-Nitro-L-arginine methyl ester hydrochloride

MAP: Mitogen-activated protein kinases

mETC: Mitochondrial electron transport chain

Min: Minute/minutes

MMPs: Matrix metalloproteinases

MPTP: Mitochondrial permeability transition pore

MTT: 3-(4,5-dimethylthiazol-2-yl)-2,5-diphenyltetrazolium bromide

NADPH: Nicotinamide adenine dinucleotide phosphate

nNOS or NOS-1: Neuronal NO-synthase or NO-synthase-1

NO: Nitric oxide

NOS: NO-synthase

NOX: NADPH oxidases

Nrf2: Nuclear factor-erythroid-2-related factor 2

O_2^-: Superoxide anion

OH: Hydroxyl radical

$ONOO^-$: Peroxynitrite

PAE: Porcine aortic endothelial cells

PBS: Phosphate buffered saline

PI_3K: Phosphatidylinositol-3-kinase

PKC: Protein kinase C

PLC: Phospholipase C

PTH: Parathyroid hormone

R.p.m.: Revolutions per minute

RANK: Receptor activator of nuclear factor-κB

RANKL: Receptor activator of nuclear factor-κB ligand

RDA: Recommended daily allowance

RI: Resistive index

RISK: Reperfusion injury salvage kinase

ROS: Reactive oxygen species

RT: Room temperature

RT-PCR: Reverse transcription-polymerase chain reaction

RXR: Retinoid X receptor

S.D.: Standard deviation

SCI: Spinal cord injury

Sec: Second/seconds

sGC: Soluble guanylate cyclase

SOD: Superoxide dismutase

SOD_1 or Cu, Zn-SOD: Copper-zinc superoxide dismutase

SOD_2 or Mn-SOD: Manganese superoxide dismutase

TGF: Transforming growth factor

TRPV6: Transient receptor potential vanilloid type 6

UVB: Ultraviolet B

VDR: Vitamin D receptor

VDREs: Vitamin D responsive elements

VEGF: Vascular endothelial growth factor

REFERENCES

1. Hopkins FG. The analyst and the medical man. Analyst. 1906; 31:385–404.

2. Allgrove J, Shaw NJ. Calcium and Bone Disorders in Children and Adolescents. 2nd, revised edition. Endocr Dev. Basel, Karger. 2015; 28:119-133. doi:10.1159/000381000.

3. Fukumoto S, Ozono K, Michigami T, Minagawa M, Okazaki R, Sugimoto T, Takeuchi Y, Matsumoto T. Pathogenesis and diagnostic criteria for rickets and osteomalacia - Proposal by an expert panel supported by Ministry of Health, Labour and Welfare, Japan, The Japanese Society for Bone and Mineral Research and The Japan Endocrine Society [Opinion]. Endocr J. 2015 Jul 4. [Epub ahead of print] PubMed PMID: 26156530.

4. Mellanby E. An experimental investigation on rickets. Lancet. 1919; 196:407–412.

5. Studies on experimental rickets. XXI. An experimental demonstration of the existence of a vitamin which promotes calcium deposition. J. Biol. Chem. 53:293–312.

6. Hess AF. The Prevention and Cure of Rickets by Sunlight. Am J Public Health (NY). 1922 Feb; 12(2):104-7. PubMed PMID: 18010639; PubMed Central PMCID: PMC1354036.

7. Windaus A, Linsert O, Luttringhaus A, Weidlinch G. Uber das krystallistierte vitamin D2. 1932; 492:226 –231.

8. Wolf G. The discovery of vitamin D: the contribution of Adolf Windaus. J Nutr. 2004 Jun; 134(6):1299-302. Erratum in: J Nutr. 2004 Aug;134(8):2015. PubMed PMID: 15173387.

9. Berridge MJ. Vitamin D cell signalling in health and disease. Biochem Biophys Res Commun. 2015 Apr 24; 460(1):53-71. doi: 10.1016/j.bbrc.2015.01.008. Review.

PubMed PMID: 25998734.

10. Bendik I, Friedel A, Roos FF, Weber P, Eggersdorfer M. Vitamin D: a critical and essential micronutrient for human health. Front Physiol. 2014 Jul 11; 5:248. doi: 10.3389/fphys.2014.00248. eCollection 2014. Review. PubMed PMID: 25071593; PubMed Central PMCID: PMC4092358.

11. Bouvard B, Annweiler C, Sallé A, Beauchet O, Chappard D, Audran M, Legrand E. Extraskeletal effects of vitamin D: facts, uncertainties, and controversies. Joint Bone Spine. 2011 Jan; 78(1):10-6. doi: 10.1016/j.jbspin.2010.10.011. Epub 2010 Dec 18. Review. PubMed PMID: 21169046.

12. Wacker M, Holick MF. Vitamin D - effects on skeletal and extraskeletal health and the need for supplementation. Nutrients. 2013 Jan 10; 5(1):111-48. doi:10.3390/nu5010111. Review. PubMed PMID: 23306192; PubMed Central PMCID: PMC3571641.

13. Girgis CM, Clifton-Bligh RJ, Hamrick MW, Holick MF, Gunton JE. The roles of vitamin D in skeletal muscle: form, function, and metabolism. Endocr Rev. 2013 Feb; 34(1):33-83. doi: 10.1210/er.2012-1012. Epub 2012 Nov 20. Review. PubMed PMID: 23169676

14. Strange RC, Shipman KE, Ramachandran S. Metabolic syndrome: A review of the role of vitamin D in mediating susceptibility and outcome. World J Diabetes. 2015 Jul 10; 6(7):896-911. doi: 10.4239/wjd.v6.i7.896. Review. PubMed PMID: 26185598; PubMed Central PMCID: PMC4499524.

15. Wu X, Zhou T, Cao N, Ni J, Wang X. Role of Vitamin D Metabolism and Activity on Carcinogenesis. Oncol Res. 2015; 22(3):129-37. doi:10.3727/096504015X14267282610894. PubMed PMID: 26168131.

16. Gröber U, Spitz J, Reichrath J, Kisters K, Holick MF. Vitamin D: Update 2013: From rickets prophylaxis to general preventive healthcare. Dermatoendocrinol. 2013 Jun 1;

5(3):331-47. doi: 10.4161/derm.26738. Epub 2013 Nov 5. Review. PubMed PMID: 24516687; PubMed Central PMCID: PMC3908963.

17. Vaishya R, Vijay V, Agarwal AK, Jahangir J. Resurgence of vitamin D: Old wine in new bottle. J Clin Orthop Trauma. 2015 Sep; 6(3):173-83. doi:10.1016/j.jcot.2015.02.002. Epub 2015 Mar 26. Review. PubMed PMID: 26155053; PubMed Central PMCID: PMC4488032.

18. Collins ED, Norman, AW. "Vitamin D" in Handbook of Vitamins. Eds Rucker RB, Suttie JW, Mccormick DB, Machlin LJ (New York, NY: Marcel Dekker Inc.). 2001; 51–113.

19. Holick MF. "Photobiology of Vitamin D" in Vitamin D. 3rd Edn., eds Feldman D, Pike JW, Adams JS (London, GB: Elsevier). 2011; 13–22.

20. Bosworth CR, Levin G, Robinson-Cohen C, Hoofnagle AN, Ruzinski J, Young B, Schwartz SM, Himmelfarb J, Kestenbaum B, de Boer IH. The serum 24,25-dihydroxyvitamin D concentration, a marker of vitamin D catabolism, is reduced in chronic kidney disease. Kidney Int. 2012 Sep; 82(6):693-700. doi:10.1038/ki.2012.193. Epub 2012 May 30. PubMed PMID: 22648296; PubMed Central PMCID: PMC3434313.

21. Bikle DD. Vitamin D metabolism, mechanism of action, and clinical applications. Chem Biol. 2014 Mar 20; 21(3):319-29. doi:10.1016/j.chembiol.2013.12.016. Epub 2014 Feb 13. Review. PubMed PMID: 24529992; PubMed Central PMCID: PMC3968073.

22. Rochel N, Wurtz JM, Mitschler A, Klaholz B, Moras D. The crystal structure of the nuclear receptor for vitamin D bound to its natural ligand. Mol Cell. 2000 Jan; 5(1):173-9. PubMed PMID: 10678179.

23. Takeshita A, Ozawa Y, Chin WW. Nuclear receptor coactivators facilitate vitamin D receptor homodimer action on direct repeat hormone response elements.

Endocrinology. 2000 Mar; 141(3):1281-4. PubMed PMID: 10698207.

24. Long MD, Sucheston-Campbell LE, Campbell MJ. Vitamin D receptor and RXR in the post-genomic era. J Cell Physiol. 2015 Apr; 230(4):758-66. doi:10.1002/jcp.24847. Review. PubMed PMID: 25335912.

25. Dampf Stone A, Batie SF, Sabir MS, Jacobs ET, Lee JH, Whitfield GK, Haussler MR, Jurutka PW. Resveratrol potentiates vitamin D and nuclear receptor signaling. J Cell Biochem. 2015 Jun; 116(6):1130-43. doi:10.1002/jcb.25070. PubMed PMID: 25536521.

26. Doig CL, Singh PK, Dhiman VK, Thorne JL, Battaglia S, Sobolewski M, Maguire O, O'Neill LP, Turner BM, McCabe CJ, Smiraglia DJ, Campbell MJ. Recruitment of NCOR1 to VDR target genes is enhanced in prostate cancer cells and associates with altered DNA methylation patterns. Carcinogenesis. 2013 Feb; 34(2):248-56. doi:10.1093/carcin/bgs331. Epub 2012 Oct 20. PubMed PMID: 23087083; PubMed Central PMCID: PMC3564435.

27. Gynther P, Toropainen S, Matilainen JM, Seuter S, Carlberg C, Väisänen S. Mechanism of 1α,25-dihydroxyvitamin D(3)-dependent repression of interleukin-12B. Biochim Biophys Acta. 2011 May; 1813(5):810-8. doi:10.1016/j.bbamcr.2011.01.037. Epub 2011 Feb 18. PubMed PMID: 21310195.

28. Polly P, Herdick M, Moehren U, Baniahmad A, Heinzel T, Carlberg C. VDR-Alien: a novel, DNA-selective vitamin D(3) receptor-corepressor partnership. FASEB J. 2000 Jul; 14(10):1455-63. PubMed PMID: 10877839.

29. Cui M, Klopot A, Jiang Y, Fleet JC. The effect of differentiation on 1,25 dihydroxyvitamin D-mediated gene expression in the enterocyte-like cell line, Caco-2. J Cell Physiol. 2009 Jan; 218(1):113-21. doi:10.1002/jcp.21574. PubMed PMID: 18726998; PubMed Central PMCID: PMC2577712.

30. Scsucova S, Palacios D, Savignac M, Mellström B, Naranjo JR, Aranda A. The

repressor DREAM acts as a transcriptional activator on Vitamin D and retinoic acid response elements. Nucleic Acids Res. 2005 Apr 22; 33(7):2269-79. Print 2005. PubMed PMID: 15849313; PubMed Central PMCID: PMC1084319.

31. Wang F, Marshall CB, Ikura M. Transcriptional/epigenetic regulator CBP/p300 in tumorigenesis: structural and functional versatility in target recognition. Cell Mol Life Sci. 2013 Nov; 70(21):3989-4008. doi:10.1007/s00018-012-1254-4. Epub 2013 Jan 11. Review. PubMed PMID: 23307074.

32. Baudino TA, Kraichely DM, Jefcoat SC Jr, Winchester SK, Partridge NC, MacDonald PN. Isolation and characterization of a novel coactivator protein, NCoA-62, involved in vitamin D-mediated transcription. J Biol Chem. 1998 Jun 26; 273(26):16434-41. PubMed PMID: 9632709.

33. Sarruf DA, Iankova I, Abella A, Assou S, Miard S, Fajas L. Cyclin D3 promotes adipogenesis through activation of peroxisome proliferator-activated receptor gamma. Mol Cell Biol. 2005 Nov; 25(22):9985-95. PubMed PMID: 16260612; PubMed Central PMCID: PMC1280250.

34. Nemere I, Dormanen MC, Hammond MW, Okamura WH, Norman AW. Identification of a specific binding protein for 1 alpha,25-dihydroxyvitamin D3 in basal-lateral membranes of chick intestinal epithelium and relationship to transcaltachia. J Biol Chem. 1994 Sep 23; 269(38):23750-6. PubMed PMID: 8089147.

35. Haussler MR, Jurutka PW, Mizwicki M, Norman AW. Vitamin D receptor (VDR)-mediated actions of 1α,25(OH)$_2$vitamin D$_3$: genomic and non-genomic mechanisms. Best Pract Res Clin Endocrinol Metab. 2011 Aug; 25(4):543-59. doi:10.1016/j.beem.2011.05.010. Review. PubMed PMID: 21872797.

36. Huhtakangas JA, Olivera CJ, Bishop JE, Zanello LP, Norman AW. The vitamin D receptor is present in caveolae-enriched plasma membranes and binds 1 alpha,25(OH)2-vitamin D3 in vivo and in vitro. Mol Endocrinol. 2004 Nov; 18(11):2660-71. Epub 2004 Jul 22. PubMed PMID: 15272054.

37. Baran DT, Quail JM, Ray R, Leszyk J, Honeyman T. Annexin II is the membrane receptor that mediates the rapid actions of 1,25-dihydroxyvitamin D3. J Cell Biochem. 2000; 78:34-46.

38. Mizwicki MT, Bishop JE, Olivera CJ, Huhtakangas JA, Norman AW. Evidence that annexin II is not a putative membrane receptor for 1,25(OH)2-vitamin D3. J Cell Biochem. 2004; 91: 852–863.

39. Vaishya R, Vijay V, Agarwal AK, Jahangir J. Resurgence of vitamin D: Old wine in new bottle. J Clin Orthop Trauma. 2015 Sep; 6(3):173-83. doi:10.1016/j.jcot.2015.02.002. Epub 2015 Mar 26. Review. PubMed PMID: 26155053; PubMed Central PMCID: PMC4488032.

40. Bendik I, Friedel A, Roos FF, Weber P, Eggersdorfer M. Vitamin D: a critical and essential micronutrient for human health. Front Physiol. 2014 Jul 11; 5:248. doi:10.3389/fphys.2014.00248. eCollection 2014. Review. PubMed PMID: 25071593; PubMed Central PMCID: PMC4092358).

41. Institute of Medicine, F.A.N.B. Dietary Reference Intakes for Calcium and Vitamin D. The National Academies Press, Washington, DC. 2011.

42. Biesalski HK. International congress 'Hidden Hunger', March 5-9, 2013, Stuttgart-Hohenheim, Germany. Ann Nutr Metab. 2013; 62(4):298-302. doi:10.1159/000351078. Epub 2013 May 30. PubMed PMID: 23735888.

43. Hilger J, Friedel A, Herr R, Rausch T, Roos F, Wahl DA, Pierroz DD, Weber P, Hoffmann K. A systematic review of vitamin D status in populations worldwide. Br J Nutr. 2014 Jan 14; 111(1):23-45. doi:10.1017/S0007114513001840. Epub 2013 Aug 9. Review. PubMed PMID: 23930771.

44. Holick MF, Chen TC. Vitamin D deficiency: a worldwide problem with health consequences. Am J Clin Nutr. 2008 Apr; 87(4):1080S-6S. Review. PubMed PMID: 18400738.

45. Mithal A, Wahl DA, Bonjour JP, Burckhardt P, Dawson-Hughes B, Eisman JA, El-Hajj Fuleihan G, Josse RG, Lips P, Morales-Torres J; IOF Committee of Scientific Advisors (CSA) Nutrition Working Group. Global vitamin D status and determinants of hypovitaminosis D. Osteoporos Int. 2009 Nov;20(11):1807-20. doi:10.1007/s00198-009-0954-6. Epub 2009 Jun 19. Review. Erratum in: Osteoporos Int. 2009 Nov; 20(11):1821. PubMed PMID: 19543765.

46. Schöttker B, Jorde R, Peasey A, Thorand B, Jansen EH, Groot Ld, Streppel M, Gardiner J, Ordóñez-Mena JM, Perna L, Wilsgaard T, Rathmann W, Feskens E, Kampman E, Siganos G, Njølstad I, Mathiesen EB, Kubínová R, Pająk A, Topor-Madry R, Tamosiunas A, Hughes M, Kee F, Bobak M, Trichopoulou A, Boffetta P, Brenner H; Consortium on Health and Ageing: Network of Cohorts in Europe and the United States. Vitamin D and mortality: meta-analysis of individual participant data from a large consortium of cohort studies from Europe and the United States. BMJ. 2014 Jun 17; 348:g3656. doi:10.1136/bmj.g3656. PubMed PMID: 24938302; PubMed Central PMCID: PMC4061380).

47. Dusso AS, Brown AJ, Slatopolsky E. Vitamin D. Am J Physiol Renal Physiol. 2005 Jul; 289(1):F8-28. Review. PubMed PMID: 15951480.

48. Christakos S. Recent advances in our understanding of 1,25-dihydroxyvitamin D(3) regulation of intestinal calcium absorption. Arch Biochem Biophys. 2012 Jul 1; 523(1):73-6. doi:10.1016/j.abb.2011.12.020. Epub 2012 Jan 2. Review. PubMed PMID: 22230327; PubMed Central PMCID: PMC3339283.

49. DeLuca HF. Overview of general physiologic features and functions of vitamin D. Am J Clin Nutr. 2004 Dec; 80(6 Suppl):1689S-96S. Review. PubMed PMID: 15585789.

50. Bouvard B, Annweiler C, Sallé A, Beauchet O, Chappard D, Audran M, Legrand E. Extraskeletal effects of vitamin D: facts, uncertainties, and controversies. Joint Bone Spine. 2011 Jan; 78(1):10-6. doi:10.1016/j.jbspin.2010.10.011. Epub 2010 Dec 18. Review. PubMed PMID: 21169046.

51. Alberts B, Johnson A, Lewis J, Morgan D, Raff M, Roberts K, Walter P. Blood Vessels and Endothelial Cells. Molecular Biology of the Cell. 4th edition. Garland Science, NY; 2002. Available from: http://www.ncbi.nlm.nih.gov/books/NBK26848/.

52. Félétou M. The Endothelium: Part 1: Multiple Functions of the Endothelial Cells - Focus on Endothelium-Derived Vasoactive Mediators. San Rafael (CA): Morgan & Claypool Life Sciences; 2011. Available from: http://www.ncbi.nlm.nih.gov/books/NBK57150/.

53. Park KH, Park WJ. Endothelial Dysfunction: Clinical Implications in Cardiovascular Disease and Therapeutic Approaches. J Korean Med Sci. 2015 Sep; 30(9):1213-25. doi:10.3346/jkms.2015.30.9.1213. Epub 2015 Aug 13. Review. PubMed PMID: 26339159; PubMed Central PMCID: PMC4553666.

54. Shu X, Keller TC 4th, Begandt D, Butcher JT, Biwer L, Keller AS, Columbus L, Isakson BE. Endothelial nitric oxide synthase in the microcirculation. Cell Mol Life Sci. 2015 Aug 25. [Epub ahead of print] PubMed PMID: 26390975.

55. Stuehr DJ, Santolini J, Wang ZQ, Wei CC, Adak S. Update on mechanism and catalytic regulation in the NO synthases. J Biol Chem. 2004 Aug 27; 279(35):36167-70. Epub 2004 May 7. Review. PubMed PMID: 15133020.

56. Thomas DD, Ridnour LA, Isenberg JS, Flores-Santana W, Switzer CH, Donzelli S, Hussain P, Vecoli C, Paolocci N, Ambs S, Colton CA, Harris CC, Roberts DD, Wink DA. The chemical biology of nitric oxide: implications in cellular signaling. Free Radic Biol Med. 2008 Jul 1; 45(1):18-31. doi:10.1016/j.freeradbiomed.2008.03.020. Epub 2008 Apr 4. Review. PubMed PMID: 18439435; PubMed Central PMCID: PMC2572721.

57. Dudzinski DM, Michel T. Life history of eNOS: partners and pathways. Cardiovasc Res. 2007 Jul 15;75(2):247-60. Epub 2007 Apr 3. Review. PubMed PMID: 17466957; PubMed Central PMCID: PMC2682334.

58. Gonzalez E, Kou R, Michel T. Rac1 modulates sphingosine 1-phosphate-mediated activation of phosphoinositide 3-kinase/Akt signaling pathways in vascular endothelial cells. J Biol Chem. 2006 Feb 10; 281(6):3210-6. Epub 2005 Dec 8. PubMed PMID: 16339142.

59. Butler AR. 'The heart less bounding': treating angina pectoris. J R Coll Physicians Edinb. 2006 Jun; 36(2):185-9. PubMed PMID: 17153155.

60. Brevetti G, Schiano V, Chiariello M. Endothelial dysfunction: a key to the pathophysiology and natural history of peripheral arterial disease? Atherosclerosis. 2008 Mar; 197(1):1-11. Review. PubMed PMID: 18076886.

61. Hill BG, Dranka BP, Bailey SM, Lancaster JR Jr, Darley-Usmar VM. What part of NO don't you understand? Some answers to the cardinal questions in nitric oxide biology. J Biol Chem. 2010 Jun 25; 285(26):19699-704. doi:10.1074/jbc.R110.101618. Epub 2010 Apr 21. Review. PubMed PMID: 20410298; PubMed Central PMCID: PMC2888379.

62. Salisbury D, Bronas U. Reactive oxygen and nitrogen species: impact on endothelial dysfunction. Nurs Res. 2015 Jan-Feb; 64(1):53-66. doi:10.1097/NNR.0000000000000068. Review. PubMed PMID: 25502061.

63. Thomas DD, Espey MG, Ridnour LA, Hofseth LJ, Mancardi D, Harris CC, Wink DA. Hypoxic inducible factor 1alpha, extracellular signal-regulated kinase, and p53 are regulated by distinct threshold concentrations of nitric oxide. Proc Natl Acad Sci U S A. 2004 Jun 15; 101(24):8894-9. Epub 2004 Jun 3. PubMed PMID: 15178764; PubMed Central PMCID: PMC428443.

64. Dan Dunn J, Alvarez LA, Zhang X, Soldati T. Reactive oxygen species and mitochondria: A nexus of cellular homeostasis. Redox Biol. 2015 Sep 10; 6:472-485. doi:10.1016/j.redox.2015.09.005. [Epub ahead of print] Review. PubMed PMID: 26432659.

65. Chen Y, Azad MB, Gibson SB. Superoxide is the major reactive oxygen species regulating autophagy. Cell Death Differ. 2009 Jul; 16(7):1040-52. doi:10.1038/cdd.2009.49. Epub 2009 May 1. PubMed PMID: 19407826.

66. Devasagayam TP, Tilak JC, Boloor KK, Sane KS, Ghaskadbi SS, Lele RD. Free radicals and antioxidants in human health: current status and future prospects. J Assoc Physicians India. 2004 Oct; 52:794-804. Review. PubMed PMID: 15909857.

67. Patel RP, Cornwell T, Darley-Usmar VM. The biochemistry of nitric oxide and peroxynitrite: implications for mitochondrial function. In: Understanding the process of ageing: The roles of mitochondria, free radicals, and antioxidants. Marcel Dekker, Inc.; NY, Basel: 1999; 39–40.

68. Coutinho T, Rooke TW, Kullo IJ. Arterial dysfunction and functional performance in patients with peripheral artery disease: a review. Vasc Med. 2011 Jun; 16(3):203-11. doi:10.1177/1358863X11400935. Epub 2011 Mar 29. Review. PubMed PMID: 21447607.

69. Deanfield JE, Halcox JP, Rabelink TJ. Endothelial function and dysfunction: testing and clinical relevance. Circulation. 2007 Mar 13; 115(10):1285-95. Review. PubMed PMID: 17353456.

70. Molinari C, Uberti F, Grossini E, Vacca G, Carda S, Invernizzi M, Cisari C. 1α,25-dihydroxycholecalciferol induces nitric oxide production in cultured endothelial cells. Cell Physiol Biochem. 2011; 27(6):661-8. doi:10.1159/000330075. Epub 2011 Jun 17. PubMed PMID: 21691084.

71. Jaffe EA, Nachman RL, Becker CG, Minick CR. Culture of human endothelial cells derived from umbilical veins. Identification by morphologic and immunologic criteria. J Clin Invest. 1973 Nov; 52(11):2745-56. PubMed PMID: 4355998; PubMed Central PMCID: PMC302542.

72. Murohara T, Witzenbichler B, Spyridopoulos I, Asahara T, Ding B, Sullivan A, Losordo DW, Isner JM. Role of endothelial nitric oxide synthase in endothelial cell migration. Arterioscler Thromb Vasc Biol. 1999 May; 19(5):1156-61. PubMed PMID: 10323764.

73. Lohr NL, Ninomiya JT, Warltier DC, Weihrauch D. Far red/near infrared light treatment promotes femoral artery collateralization in the ischemic hindlimb. J Mol Cell Cardiol. 2013 Sep; 62:36-42. doi:10.1016/j.yjmcc.2013.05.007. Epub 2013 May 20. PubMed PMID: 23702287; PubMed Central PMCID: PMC3747970.

74. Sun HY, Wang NP, Kerendi F, Halkos M, Kin H, Guyton RA, Vinten-Johansen J, Zhao ZQ. Hypoxic postconditioning reduces cardiomyocyte loss by inhibiting ROS generation and intracellular Ca2+ overload. Am J Physiol Heart Circ Physiol. 2005 Apr; 288(4):H1900-8. Epub 2004 Nov 24. PubMed PMID: 15563525.

75. Förster K, Paul I, Solenkova N, Staudt A, Cohen MV, Downey JM, Felix SB, Krieg T. NECA at reperfusion limits infarction and inhibits formation of the mitochondrial permeability transition pore by activating p70S6 kinase. Basic Res Cardiol. 2006 Jul; 101(4):319-26. Epub 2006 Apr 8. PubMed PMID: 16604438.

76. Dedkova EN, Blatter LA. Characteristics and function of cardiac mitochondrial nitric oxide synthase. J Physiol. 2009 Feb 15; 587(Pt 4):851-72. doi:10.1113/jphysiol.2008.165423. Epub 2008 Dec 22. PubMed PMID: 19103678; PubMed Central PMCID: PMC2669975.

77. Uberti F, Caimmi PP, Molinari C, Mary D, Vacca G, Grossini E. Levosimendan modulates programmed forms of cell death through K(ATP) channels and nitric oxide. J Cardiovasc Pharmacol. 2011 Feb; 57(2):246-58. doi:10.1097/FJC.0b013e318204bb55. PubMed PMID: 21107279.

78. Layman H, Spiga MG, Brooks T, Pham S, Webster KA, Andreopoulos FM. The effect of the controlled release of basic fibroblast growth factor from ionic gelatin-based hydrogels on angiogenesis in a murine critical limb ischemic model. Biomaterials.

2007 Jun; 28(16):2646-54. Epub 2007 Feb 12. PubMed PMID: 17320947; PubMed Central PMCID: PMC1945227.

79. Renò F, Rizzi M, Cannas M. Gelatin-based anionic hydrogel as biocompatible substrate for human keratinocyte growth. J Mater Sci Mater Med. 2012 Feb; 23(2):565-71. doi:10.1007/s10856-011-4519-9. Epub 2011 Dec 13. PubMed PMID: 22160746.

80. Braam LA, Hoeks AP, Brouns F, Hamulyák K, Gerichhausen MJ, Vermeer C. Beneficial effects of vitamins D and K on the elastic properties of the vessel wall in postmenopausal women: a follow-up study. Thromb Haemost. 2004 Feb; 91(2):373-80. PubMed PMID: 14961167.

81. Barreto DV, Barreto FC, Liabeuf S, Temmar M, Boitte F, Choukroun G, Fournier A, Massy ZA. Vitamin D affects survival independently of vascular calcification in chronic kidney disease. Clin J Am Soc Nephrol. 2009 Jun; 4(6):1128-35. doi:10.2215/CJN.00260109. Epub 2009 May 14. PubMed PMID: 19443628; PubMed Central PMCID: PMC2689889.

82. Wong MS, Leisegang MS, Kruse C, Vogel J, Schürmann C, Dehne N, Weigert A, Herrmann E, Brüne B, Shah AM, Steinhilber D, Offermanns S, Carmeliet G, Badenhoop K, Schröder K, Brandes RP. Vitamin D promotes vascular regeneration. Circulation. 2014 Sep 16; 130(12):976-86. doi:10.1161/CIRCULATIONAHA.114.010650. Epub 2014 Jul 11. PubMed PMID: 25015343.

83. Cooke JP. NO and angiogenesis. Atheroscler Suppl. 2003 Dec; 4(4):53-60. Review. PubMed PMID: 14664903.

84. Adya R, Tan BK, Punn A, Chen J, Randeva HS. Visfatin induces human endothelial VEGF and MMP-2/9 production via MAPK and PI3K/Akt signalling pathways: novel insights into visfatin-induced angiogenesis. Cardiovasc Res. 2008 May 1; 78(2):356-65. Epub 2007 Dec 18. PubMed PMID: 18093986.

85. Brown J, Reading SJ, Jones S, Fitchett CJ, Howl J, Martin A, Longland CL, Michelangeli F, Dubrova YE, Brown CA. Critical evaluation of ECV304 as a human endothelial cell model defined by genetic analysis and functional responses: a comparison with the human bladder cancer derived epithelial cell line T24/83. Lab Invest. 2000 Jan; 80(1):37-45. PubMed PMID: 10653001.

86. Rasente RY, Egitto P, Calabrese GC. Low molecular mass dermatan sulfate modulates endothelial cells proliferation and migration. Carbohydr Res. 2012 Jul 15; 356:233-7. doi:10.1016/j.carres.2012.03.036. Epub 2012 Apr 5. PubMed PMID: 22533918.

87. Gao H, Zhang J, Liu T, Shi W. Rapamycin prevents endothelial cell migration by inhibiting the endothelial-to-mesenchymal transition and matrix metalloproteinase-2 and -9: an in vitro study. Mol Vis. 2011; 17:3406-14. Epub 2011 Dec 24. PubMed PMID: 22219636; PubMed Central PMCID: PMC3247170).

88. Rundhaug JE. Matrix metalloproteinases and angiogenesis. J Cell Mol Med. 2005 Apr-Jun; 9(2):267-85. Review. PubMed PMID: 15963249.

89. Kiran MS, Sameer Kumar VB, Viji RI, Sudhakaran PR. Temporal relationship between MMP production and angiogenic process in HUVECs. Cell Biol Int. 2006 Sep; 30(9):704-13. Epub 2006 May 10. PubMed PMID: 16829143).

90. Cavdar Z, Oktay G, Egrilmez MY, Genc S, Genc K, Altun Z, Islekel H, Guner G. In vitro reoxygenation following hypoxia increases MMP-2 and TIMP-2 secretion by human umbilical vein endothelial cells. Acta Biochim Pol. 2010; 57(1):69-73. Epub 2010 Mar 10. PubMed PMID: 20216978.

91. Li H, Daculsi R, Bareille R, Bourget C, Amedee J. uPA and MMP-2 were involved in self-assembled network formation in a two dimensional co-culture model of bone marrow stromal cells and endothelial cells. J Cell Biochem. 2013 Mar; 114(3):650-7. doi:10.1002/jcb.24407. PubMed PMID: 23059760.

92. Ikeda Y, Aihara K, Yoshida S, Iwase T, Tajima S, Izawa-Ishizawa Y, Kihira Y, Ishizawa K, Tomita S, Tsuchiya K, Sata M, Akaike M, Kato S, Matsumoto T, Tamaki T. Heparin cofactor II, a serine protease inhibitor, promotes angiogenesis via activation of the AMP-activated protein kinase-endothelial nitric-oxide synthase signaling pathway. J Biol Chem. 2012 Oct 5; 287(41):34256-63. doi:10.1074/jbc.M112.353532. Epub 2012 Aug 17. PubMed PMID: 22904320; PubMed Central PMCID: PMC3464533.

93. Coletta C, Papapetropoulos A, Erdelyi K, Olah G, Módis K, Panopoulos P, Asimakopoulou A, Gerö D, Sharina I, Martin E, Szabo C. Hydrogen sulfide and nitric oxide are mutually dependent in the regulation of angiogenesis and endothelium-dependent vasorelaxation. Proc Natl Acad Sci U S A. 2012 Jun 5; 109(23):9161-6. doi:10.1073/pnas.1202916109. Epub 2012 May 8. PubMed PMID: 22570497; PubMed Central PMCID: PMC3384190.

94. Mujoo K, Krumenacker JS, Murad F. Nitric oxide-cyclic GMP signaling in stem cell differentiation. Free Radic Biol Med. 2011 Dec 15; 51(12):2150-7. doi:10.1016/j.freeradbiomed.2011.09.037. Epub 2011 Oct 6. Review. PubMed PMID: 22019632; PubMed Central PMCID: PMC3232180.

95. Polidoro L, Properzi G, Marampon F, Gravina GL, Festuccia C, Di Cesare E, Scarsella L, Ciccarelli C, Zani BM, Ferri C. Vitamin D protects human endothelial cells from H2O2 oxidant injury through the Mek/Erk-Sirt1 axis activation. J Cardiovasc Transl Res. 2013 Apr; 6(2):221-31. doi:10.1007/s12265-012-9436-x. Epub 2012 Dec 18. PubMed PMID: 23247634.

96. Razavi HM, Hamilton JA, Feng Q. Modulation of apoptosis by nitric oxide: implications in myocardial ischemia and heart failure. Pharmacol Ther. 2005 May; 106(2):147-62. Epub 2005 Jan 12. Review. PubMed PMID: 15866317.

97. Foncea R, Carvajal C, Almarza C, Leighton F. Endothelial cell oxidative stress and signal transduction. Biol Res. 2000; 33(2):89-96. PubMed PMID: 15693275.

98. Antoniades C, Tousoulis D, Tentolouris C, Toutouzas P, Stefanadis C. Oxidative stress, antioxidant vitamins, and atherosclerosis. From basic research to clinical practice. Herz. 2003 Nov; 28(7):628-38. Review. PubMed PMID: 14689123.

99. Pestana CR, Silva CH, Uyemura SA, Santos AC, Curti C. Impact of adenosine nucleotide translocase (ANT) proline isomerization on Ca2+-induced cysteine relative mobility/mitochondrial permeability transition pore. J Bioenerg Biomembr. 2010 Aug; 42(4):329-35. doi:10.1007/s10863-010-9297-4. Epub 2010 Jul 8. PubMed PMID: 20614171.

100. Kwon SH, Pimentel DR, Remondino A, Sawyer DB, Colucci WS. H2O2 regulates cardiac myocyte phenotype via concentration-dependent activation of distinct kinase pathways. J Mol Cell Cardiol. 2003 Jun; 35(6):615-21. PubMed PMID: 12788379.

101. Han H, Long H, Wang H, Wang J, Zhang Y, Wang Z. Progressive apoptotic cell death triggered by transient oxidative insult in H9c2 rat ventricular cells: a novel pattern of apoptosis and the mechanisms. Am J Physiol Heart Circ Physiol. 2004 Jun; 286(6):H2169-82. Epub 2004 Jan 22. PubMed PMID: 14739138.

102. Rizzuto R, Pozzan T. Microdomains of intracellular Ca2+: molecular determinants and functional consequences. Physiol Rev. 2006 Jan; 86(1):369-408. Review. PubMed PMID: 16371601.

103. Carelli S, Giallongo T, Gerace C, De Angelis A, Basso MD, Di Giulio AM, Gorio A. Neural stem cell transplantation in experimental contusive model of spinal cord injury. J Vis Exp. 2014 Dec 17; (94). doi:10.3791/52141. PubMed PMID: 25548937.

104. Morse LR, Battaglino RA, Stolzmann KL, Hallett LD, Waddimba A, Gagnon D, Lazzari AA, Garshick E. Osteoporotic fractures and hospitalization risk in chronic spinal cord injury. Osteoporos Int. 2009 Mar; 20(3):385-92. doi:10.1007/s00198-008-0671-6. Epub 2008 Jun 26. PubMed PMID: 18581033; PubMed Central PMCID: PMC2640446.

105. Morse LR, Sudhakar S, Danilack V, Tun C, Lazzari A, Gagnon DR, Garshick E, Battaglino RA. Association between sclerostin and bone density in chronic spinal cord injury. J Bone Miner Res. 2012 Feb; 27(2):352-9. doi:10.1002/jbmr.546. PubMed PMID: 22006831; PubMed Central PMCID: PMC3288145.

106. Morse LR, Sudhakar S, Lazzari AA, Tun C, Garshick E, Zafonte R, Battaglino RA. Sclerostin: a candidate biomarker of SCI-induced osteoporosis. Osteoporos Int. 2013 Mar; 24(3):961-8. doi:10.1007/s00198-012-2072-0. Epub 2012 Jul 17. PubMed PMID: 22801952; PubMed Central PMCID: PMC3611240.

107. Schoenau E. From mechanostat theory to development of the "Functional Muscle-Bone-Unit". J Musculoskelet Neuronal Interact. 2005 Jul-Sep; 5(3):232-8. Review. PubMed PMID: 16172514.

108. Cianferotti L, Brandi ML. Muscle-bone interactions: basic and clinical aspects. Endocrine. 2014 Mar; 45(2):165-77. doi:10.1007/s12020-013-0026-8. Epub 2013 Aug 29. Review. PubMed PMID: 23990248.

109. Mo C, Romero-Suarez S, Bonewald L, Johnson M, Brotto M. Prostaglandin E2: fromclinical applications to its potential role in bone- muscle crosstalk and myogenic differentiation. Recent Pat Biotechnol. 2012 Dec; 6(3):223-9. PubMed PMID: 23092433; PubMed Central PMCID: PMC3732468.

110. American Spinal Injury Association. International Standards for Neurological Classification of Spinal Cord Injury. Revised 2011. American Spinal Injury Association: Atlanta, GA, USA.

111. Ditunno JF Jr, Young W, Donovan WH, Creasey G. The international standards booklet for neurological and functional classification of spinal cord injury. American Spinal Injury Association. Paraplegia. 1994 Feb; 32(2):70-80. PubMed PMID: 8015848.

112. Kirshblum SC, Memmo P, Kim N, Campagnolo D, Millis S; American Spinal Injury

Association. Comparison of the revised 2000 American Spinal Injury Association classification standards with the 1996 guidelines. Am J Phys Med Rehabil. 2002 Jul; 81(7):502-5. PubMed PMID: 12131176.

113. Invernizzi M, Carda S, Milani P, Mattana F, Fletzer D, Iolascon G, Gimigliano F, Cisari C. Development and validation of the Italian version of the Spinal Cord Independence Measure III. Disabil Rehabil. 2010; 32(14):1194-203. doi:10.3109/09638280903437246. PubMed PMID: 20131944.

114. Kyle UG, Genton L, Hans D, Pichard C. Validation of a bioelectrical impedance analysis equation to predict appendicular skeletal muscle mass (ASMM). Clin Nutr. 2003 Dec; 22(6):537-43. PubMed PMID: 14613755.

115. Gilks CB, Prat J. Ovarian carcinoma pathology and genetics: recent advances. Hum Pathol. 2009 Sep; 40(9):1213-23. doi:10.1016/j.humpath.2009.04.017. Epub 2009 Jun 24. Review. PubMed PMID: 19552940.

116. Sankaranarayanan R, Ferlay J. Worldwide burden of gynaecological cancer: the size of the problem. Best Pract Res Clin Obstet Gynaecol. 2006 Apr; 20(2):207-25. Epub 2005 Dec 13. Review. PubMed PMID: 16359925.

117. Jemal A, Siegel R, Ward E, Hao Y, Xu J, Murray T, Thun MJ. Cancer statistics, 2008. CA Cancer J Clin. 2008 Mar-Apr; 58(2):71-96. doi:10.3322/CA.2007.0010. Epub 2008 Feb 20. PubMed PMID: 18287387.

118. Vercellini P, Crosignani P, Somigliana E, Viganò P, Buggio L, Bolis G, Fedele L. The 'incessant menstruation' hypothesis: a mechanistic ovarian cancer model with implications for prevention. Hum Reprod. 2011 Sep; 26(9):2262-73. doi:10.1093/humrep/der211. Epub 2011 Jun 30. PubMed PMID: 21724568.

119. Kurman RJ. Origin and molecular pathogenesis of ovarian high-grade serous carcinoma. Ann Oncol. 2013 Dec; 24 Suppl 10:x16-21. doi:10.1093/annonc/mdt463. Review. PubMed PMID: 24265397.

120. Kuhn E, Ayhan A, Shih IeM, Seidman JD, Kurman RJ. Ovarian Brenner tumour: a morphologic and immunohistochemical analysis suggesting an origin from fallopian tube epithelium. Eur J Cancer. 2013 Dec; 49(18):3839-49. doi:10.1016/j.ejca.2013.08.011. Epub 2013 Sep 5. PubMed PMID: 24012099.

121. Landen CN Jr, Birrer MJ, Sood AK. Early events in the pathogenesis of epithelial ovarian cancer. J Clin Oncol. 2008 Feb 20; 26(6):995-1005. doi:10.1200/JCO.2006.07.9970. Epub 2008 Jan 14. Review. PubMed PMID: 18195328.

122. Vang R, Shih IeM, Kurman RJ. Fallopian tube precursors of ovarian low- and high-grade serous neoplasms. Histopathology. 2013 Jan; 62(1):44-58. doi:10.1111/his.12046. Review. PubMed PMID: 23240669.

123. Sherman-Baust CA, Kuhn E, Valle BL, Shih IeM, Kurman RJ, Wang TL, Amano T, Ko MS, Miyoshi I, Araki Y, Lehrmann E, Zhang Y, Becker KG, Morin PJ. A genetically engineered ovarian cancer mouse model based on fallopian tube transformation mimics human high-grade serous carcinoma development. J Pathol. 2014 Jul; 233(3):228-37. doi:10.1002/path.4353. PubMed PMID: 24652535; PubMed Central PMCID: PMC4149901.

124. Kurman RJ, Shih IeM. The origin and pathogenesis of epithelial ovarian cancer: a proposed unifying theory. Am J Surg Pathol. 2010 Mar; 34(3):433-43. doi:10.1097/PAS.0b013e3181cf3d79. PubMed PMID: 20154587; PubMed Central PMCID: PMC2841791.

125. Toyokuni S. Role of iron in carcinogenesis: cancer as a ferrotoxic disease. Cancer Sci. 2009 Jan; 100(1):9-16. doi:10.1111/j.1349-7006.2008.01001.x. Epub 2008 Oct 23. Review. PubMed PMID: 19018762.

LIST OF PUBLICATIONS

(in chronological order)

- Molinari C, Rizzi M, Squarzanti DF, Pittarella P, Vacca G, Renò F. 1α,25-Dihydroxycholecalciferol (Vitamin D3) induces NO-dependent endothelial cell proliferation and migration in a three-dimensional matrix. Cell Physiol Biochem. 2013; 31(6):815-22. doi:10.1159/000350099. Epub 2013 Jun 4. PubMed PMID: 23816836.

- Uberti F, Lattuada D, Morsanuto V, Nava U, Bolis G, Vacca G, Squarzanti DF, Cisari C, Molinari C. Vitamin D protects human endothelial cells from oxidative stress through the autophagic and survival pathways. J Clin Endocrinol Metab. 2014 Apr; 99(4):1367-74. doi:10.1210/jc.2013-2103. Epub 2013 Nov 27. PubMed PMID: 24285680.

- Lattuada D, Uberti F, Colciaghi B, Morsanuto V, Maldi E, Squarzanti DF, Molinari C, Boldorini R, Bulfoni A, Colombo P, Bolis G. Fimbrial cells exposure to catalytic iron mimics carcinogenic changes. Int J Gynecol Cancer. 2015 Mar; 25(3):389-98. doi:10.1097/IGC.0000000000000379. PubMed PMID: 25594146.

- Pittarella P, Squarzanti DF, Molinari C, Invernizzi M, Uberti F, Renò F. NO-dependent proliferation and migration induced by Vitamin D in HUVEC. J Steroid Biochem Mol Biol. 2015 May; 149:35-42. doi:10.1016/j.jsbmb.2014.12.012. Epub 2015 Jan 20. PubMed PMID: 25616003.

- Invernizzi M, Carda S, Rizzi M, Grana E, Squarzanti DF, Cisari C, Molinari C, Renò F. Evaluation of serum myostatin and sclerostin levels in chronic spinal cord injured patients. Spinal Cord. 2015 Aug; 53(8):615-20. doi:10.1038/sc.2015.61. Epub 2015 Apr 21. PubMed PMID: 25896346.